SIMULATION OF NOT-, AND- AND OR- OPTICAL GATES USING WIDEBAND TRAVELLING WAVE SEMICONDUCTOR OPTICAL AMPLIFIER

BY
NGETICH WESLEY

A THESIS SUBMITTED IN PARTIAL FULFILLMENT OF THE REQUIREMENT FOR THE AWARD OF MASTER OF SCIENCE DEGREE IN PHYSICS, SCHOOL OF SCIENCE, UNIVERSITY OF ELDORET, ELDORET, KENYA

2016

DECLARATION

DECLARATION BY THE STUDENT

This thesis is my own original work and has not been presented for a degree in any other University or Institution. No part of this thesis may be reproduced without the prior written permission of the author and the University of Eldoret.

Ngetich Wesley Signature……………..…………….. Date..……………

SC/PGP/010/2010

APPROVAL BY THE SUPERVISORS

This thesis has been submitted for examination with our approval as University Supervisors.

Dr. David W. Waswa Signature…………..………………. Date..………………
University of Eldoret,
Department of Physics
Eldoret

Prof. Joel Tonui Signature...…………..………………. Date..………………
University of Eldoret,
Department of Physics
Eldoret

DEDICATION

This research is dedicated to my dear son Emmanuel Patley Cheruiyot, my wife Chemutai Patricia Ngetich,- teacher at Masindoni Secondary School, Chepalungu , those who have inspired me and all those whom we have shared the same dream.

ABSTRACT

All optical gates have received practical applications in the recent past. This is due to its high demand in optical communication networks in this age of Information Technology (IT). They have assisted in performance of logic functions along the network such as: building of time reversals, differentiators, integrators and multiplexers. However, challenges still do exist along the communication channels such as data delay which requires automatic switches for routing, wavelength conversion, data generation and regeneration. All optical gates have been built and demonstrated using different types of Semiconductor Optical Amplifier (SOA); Travelling wave and reflective SOA to alleviate this problem. Using Optisystem software, AND, NOT and OR Optical gates were simulated using Wideband Travelling Wave Semiconductor Operational Amplifier (WTW SOA). Their setups were simulated to ascertain working characteristics. A generated pattern of signal was modulated in Mach-Zender Modulator (MZM) with 0 dBm power, 193.1 THz Continuous Wave (CW) laser through several components and fibres. At 10 Gbits, sampled bit sequences and selected injected currents and lengths of fibres and the WTW SOA, were used. The signal was generated and delayed optically along the optical fibre for a NOT gate to be realized , while it was split into two in other gates and delayed to have two overlapped input signals into the WTW SOA. It was established that the working length and current for NOT gate was 0.001 m and 0.13 A while that of AND gate was 0.003 m and 0.0003 A. The OR gate was realized at a length of 0.0000001 m and at a current of 0.0031 A. This research shows that WTW SOA produced essential optical gates at the specified lengths and injection currents. This research, if adapted, will accelerate data propagation in communication networks since all optical gates are useful in optical communication networks as they can make automatic Optical switches, data routers, multiplexers, integrators, differentiators and other combinational optical processing systems.

ACKNOWLEDGEMENT

I would like to thank my God for enabling me carry out my research to the end free from health problems. His name be exalted forever. Secondly, thanks goes to my supervisors Dr. David Waswa and Prof. Joel Tonui for their tireless work for assisting me throughout my research .Whenever I needed them; they were ready to assist me especially in learning the softwares. Special thanks go to entire University of Eldoret administration for giving me a chance to use their facilities in research. Special regards goes to my colleagues Isoe George of Nelson Mandela metropolitan University, South Africa, Osiemo D, Rono Charles of Johannes burg University, South Africa, Dr.Enoch Kirwa of department of Physics Kabianga University to mention just a few who encouraged me throughout my research. Lastly, regards goes to my best friend, my partner and only wife Chemutai Patricia Ngetich who gave me humble time, patience and encouragement for the lengthy period of my research.

TABLE OF CONTENT

LIST OF FIGURES

LIST OF ABBREVIATIONS AND SYMBOLS

ASE	Amplified Spontaneous Emission
CW	Continuous Wave
$\vec{E}$	Electric Field component
FWM	Full Wave Mixing
GaAs	Gallium Arsenide
$\vec{H}$	Magnetic field component
ICT	Information communication Technology
InP	Indium Phosphide
IP	Internet Protocol
IT	Information Technology
LAN	Local Area Network
MAN	Metropolitan Area Network
MZM	Mach-Zender Modulator
NF	Noise Figure.
O/E	Optical-Electrical
OSNR	Optical Signal To Noise Ratio
PRBS	Pseudo Random Bit Sequence
SOA	Semiconductor Optical Amplifier
SPM	Self Phase Modulation.
WAN	Wide Area Network
WDM	Wavelength Division Multiplexing

WTW SOA	Wideband Travelling Wave Semiconductor Operational Amplifier
XGM	Cross Gain Modulation
B_m	Measure of birefringence
K_0	wave vector
n	Refractive index
n_1^2	Refractive index for core
n_2^2	Refractive index for cladding
n_{cl}	Cladding refractive index
n_{co}	Core refractive index
Θ_{cr}	Critical angle
∇	Delta
λ_0	Wavelength of light
ω_0	Operating frequency
B_0	optical bandwidth of a filter
c	Velocity of light in vacuum
G	Gain
GVD	Group Velocity Dispersion
h	Planck's constant
V_g	Group Velocity
z	Fibre length
β	Phase (propagation) constant
ω	Frequency

Θ	Phase shift
$\emptyset$	Phase of wave
ξ	Angle between optical fibre axis and wave vector of light propagating in waveguide
r	Radius of fibre

CHAPTER ONE

INTRODUCTION

1.1 Background Information

Optical fibre functions have grown tremendously since its invention in the early 1970s (Agrawal, 2012). With the rise of information traffic due to the Internet, voice data, video, computer networks, electronic commerce and multimedia, the need for a transmission medium for handling such huge amounts of information with big bandwidth capabilities is paramount. Fibre optics, with its comparatively infinite bandwidth, has proven to be the solution, due to its effectiveness, speed and efficiency. The principle of light is used in fibre optic communication network because fibres can carry more information over longer distances as compared to electrical signals that carry in a copper, coaxial medium or radio frequencies through a wireless medium. In optical fibre, data can be propagated with amplification, few transmission losses, low interference, and with high bandwidth potential (Barnoski, 2012). All optical signal processing has lessened complications and cumbersomeness of electronics in data communications networks to perform logic functions within the network (Choi, 2010) (Singh, 2014.) (Son, 2007). For example, electro-optical conversions in all-optical networks: time reversals, differentiators, integrators, multiplexers, have been fully attained by use of all optical logic gates such as OR, AND, NOR, NAND and XOR gates for all-optical signal processing. These functions have been demonstrated to be working using the non linear effects of Semiconductor optical Amplifiers (SOA) because of its high speed effects (Yi, 2010). A logic gate is a device that performs logical operations depending on one or more inputs to give a single output. The concept of digital electronics is applied where the result is either "true" or "false" respectively. This is the switching mechanisms which has developed a lot of curiosity and key interest in the optics community whereas in electronics it has received a lot of challenges due to its cumbersomeness, bulkiness and cost. In fact, it is noted that logic gates in electronics use a lot of components like transistors to build on a single chip which takes more time to perform required task whereas in optical networks, it takes few components to construct it and within the fast speed of light, the task is completed. Optical gates then can assist in optical computing and optical communication networks compared to electronic networks. One of the noted advantages of optical network is immunity to short circuiting and interference. The bandwidth is also very big. It has easy, cheap parallel computing and lower loss transmission because of its components which are portable and compact within the system (Massaro, 2012).

1.2 Statement of the problem

Population increase over the years has led to more demand and faster facilities in Information Communication Technology (ICT). This has made data transmission schemes under Wavelength Division Multiplexing (WDM) in optical communication network be affected by storage capacity, computational power, real time processing, inflexibility of configuration, cumbersomeness and network level cost. Furthermore, it has led to slowed down flow of information in electro-optic communication network. This effect need data propagation from traffic jam electronic to a high speed optical network especially in areas such as LAN, WAN and MAN or even international.. However, the change of information propagation to optical form has increased internet Protocol (IP) traffic in telecommunication infrastructure.

1.3 Objectives

The general objective is to model all-optical gates in order to simplify the optical network and optically increase the effectiveness and efficiency of the network laid out for its functions. The specific objectives of this research were to;

i. To model NOT, AND and OR optical gates using Wideband Travelling Wave Semiconductor Operational Amplifier (WTW SOA).

ii. To investigate the parameters affecting Wideband Travelling Wave Semiconductor Operational Amplifier (WTW SOA) as an optical gate.

1.4 Justification of the study

Electronic data transfer has been used widely in the past century to date. In the more recent past, information transfer has been under optical communication network. All-optical gates in the modern network are very essential as they use light, little current and power for their control. They are required for high-speed logical functions in wavelength converters, data routers, optical add-drop multiplexers and optical cross connects. They perform networking functions such as clock ex-traction, packet synchronization, signal regeneration, addressing, header recognition, data encoding and encryption (Gates, 2012). This intense and accelerated growth in broadband telecommunication network access and capacity will necessitate next-generation high-performance in computing systems and internet packet routing systems to support extremely high-bandwidth traffic flows and applications. This will improve on effectiveness and efficiency of system networks. Thus, they will accelerate internet reach and hence create jobs in ICT sector as well as contributing towards realizing Kenya’s vision 2030.

CHAPTER TWO

THEORY AND LITERATURE REVIEW

2.1 Introduction

Optical data processing is the modern most successful way to overcome problems of electronic or optical-electronic data processing system. All-optical logic gates are vital components for high speed signal processing in optical communication network in the modern rising telecommunication. The optical gates eliminate the complex, bulky electro-optic conversion since they work in nonlinear characteristics of a medium which aid in performance of logic function elements such as data synchronization, wavelength converters, routers, signal regeneration, address and header recognition and signal processing. SOAs are utilized for this logic functions due to their transparency, efficiency, compactness and stability. They allow photonic integration and can control the optical gate by change of their carrier density, refractive index or optical phase shift. Light is being used in all optical domain processing since it has the characteristic of parallelism where photons are faster than the electrons. All optical logic operations require principles for encoding such as spatial, frequency, intensity, polarizations and phase which are the basis for their operations of light. Here, absence of light is encoded as “0”, and presence of light is encoded as “1”. This can be recorded in communications network as no signal, or presence of a signal. Light is key in optical communication network since it aids in super positioning and superimposing of signals which leads to formation of the all optical logical gates which are very important in logic functions and other applications in system networks namely;

1. All optical bit pattern recognition
2. All optical Bit Error Rate (BER) monitoring.
3. All optical packet address
4. Payload separation
5. All optical label swapping
6. All packet drops in optical time domain multiplexing networks (OTDM) (Li, 2005)

This has been obtained in several ways using fibre or SOA because of their efficiency and photonic integration (Guan, 2013). Many interferometric structural gates have been built depending on polarization and nonlinear effects of SOA such as cross phase modulation (XPM), self phase modulation (SPM), cross Gain modulation (XGM) and cross polarization Modulation (XPolM) at <40 GB. XGM have been used to demonstrate the functions of SOAs such as amplification, switching and wavelength conversion where they used the control of input power to affect carrier density to change the input signal. Using the SOA-based MZI, all optical logic gates are shown using various switching windows (Kaur & Kaler, 2014) Parameters such as temperature showed that larger gain for the output pulses within a shorter period limits the operation speed of the gates while moderate values of material loss coefficient are depicted to be favorable towards realization of all optical gates. The dynamic response of SOA by use of XPM where phase shift of SOA-MZI depended on enhancement factor determined the AND gate. For this purpose, cross-talk performance degradation performance and power drop is observed on longer SOA length while for moderate values of SOA such as optical signal and pulse width, the operation of a gate is improved at 10 GB. And by change of powers in lasers, and use of band pass filters (BPF) at 10 GB, SOA worked as OR and XOR gates. Though it depicted power attenuation by the filter detuning at 15 dB, the selection of strong signals was done for a better XOR gate. Fine tuning of delay lines and power factor of lasers at 20 GB led to the AND gate when two SOAs are cascaded for all optical gates (Zheng, 2012). Since there was synchronization of signals to overlap, the binary logic points of the probe and pump signals were due to variation of currents and power signals which led to gates being attained at low speed of 10 GB for small recovery time of SOA. Further demonstration has been shown under XGM at 10 GB for two SOAs for OR and NOR gate at small injection currents which excited electrons and stimulated the input signal for amplification. The SOAs had an active region of 600 μm and carrier lifetime of 800 *p*s. The Transmission Line Laser Model (TLLM) method used under VPI software showed that these gates worked under controlled pump and probe beam power of around 100 mW at proper gain saturation.

Dilute mode SOA (DSOA) has also been utilized to obtain an optical gate by varying the extinction ratio and control of current to a saturation point. The limit factor is the effective carrier life time that has been reduced by increasing of stimulated emission photon density at 100 GHz OFF state of DSOA gate. All optical multi-logic device has also been utilized using High Non-Linear Fibre (HNLF) operating at 10 GB to obtain error free performance and power penalties of 5.9 dB ,-1.0 dB and 2.9 dB for XOR, AND and OR operations respectively (Qiu, Sun, Rochette & Chen, 2010). Though SOA was not utilized here, the fibre of length 1007 m was used to obtain the optical gate. The inputs power wavelengths and polarization of BPF are varied to obtain the gates. A bigger wavelength separation of 14.0 nm was preferred here since the power could be increased to maximize the XPM. A similar approach was used for a simple structure of SOA and BPF that allowed photonic integration to realize AND, OR and XOR gates (Li et al, 2005). The length of BPF was 0.3 nm for FWHM centered at 1560 nm. In order to make optical gates, the wavelength of the probe was tuned to adjust the detuned filter so that the output power can be attenuated to more than 15 dB. The slope of the optical BPF was about 0.4 dB/GHz hence signals couldn't reach the ground level. The set up used operated at controlled inputs powers for probe and the pump. This didn't observe any patterning effect but saw small residual output pulses of the gates.

Cascaded single SOA also has been utilized for AND gate and used large input signal that resulted to better output performance (Zhang, Wang, Sun, Liu, & Huang, 2004). The SOA was fabricated with materials and had vertical active cavity of length 400 m, gain of -10 dB with biased current of 150 mA. This resulted to wavelength conversion and optical amplification. Due to its cascading, the optical AND gate power varied at different channels for the novel scheme and the increase in signal power led to trade off of output performance and output average power. Experimentally, the signal power is critical to output performance of logic function operation.

An ultrafast all optical XOR logic gate using symmetrical SOI based MZI configuration at 0.33 Tb/s was proposed also at various input optical power and SOI waveguide length (Wu & Sarma, 2010). The variation of width and height (cross-section) made SOI to undergo interferences of inputs for the gate to occur. Destructive interference led to 0 logic while constructive led to 1 logic. The output amplitude fluctuated due to Pseudo random Bit Sequence (PRBS) pattern effect. Also, walk-off effect led to shift of XOR gate signal with respect to input signal. It further used extinction ratio and the eye opening to evaluate the performance of XOR gate where they rapidly changed depending on the input optical power and waveguide length. Here, when power is increased with SOI length of 4 mm and 1.0 W input probe power, the quality of resultant eye diagram change. A strong patterning effect and slight change in carrier led to variation of output logic signal. Generally, the extinction ratio and eye opening depend strongly on non-linear processes including XPM and non degenerate two-photon absorption. This two parameters are sensitive to input powers and the waveguide length which are adjustable for quality output XOR logic gate signal. A XPM all optical wavelength converter (AOWC) composed of MZI SOA has also been used to obtain logic AND gate where suitable currents were applied to change the carrier density of each SOA before coupling in the interferometric structures(Patil, Singh, & Singh, 2014). This changed the refractive index and the phase of the probe beam in the SOA to form the output signal. Interference of the two beams altered the intensity of output signal as injected power increased. Here, the variations of intensity probe signal in the XPM AOWC and static transfer characteristics led to AND logic function of 20 GB at defined binary points.

XPM wavelength converter (Alcatel 1901 ICM) has been also used to accomplish all-optical AND gate at 20 GB/s, where input and output signals were configured (Kim et al., 2004). Due to gain saturation effect of SOA, the gate was realized. The same application has been utilized too for NOR and XOR gate at 10 GB/s. Though the XOR used XGM with two SOAs for complex logic functions such as half and full adder (Kadam & Gupta, 2012). It operated at limited speeds due to high recovery of SOA. Furthermore, for the improved functionalities such as bit extraction, optical packet switching, regeneration and decision making, the SOAs were cascaded.

Bulk SOA with passive optical filter (POF) has also been used to make NOR, XOR and NAND gates at a speed of 1 Tb/s (Sahafi, Rostami, & Sahafi, 2012). A 200 mA was used to bias the SOA and simulations for varied input optical signal were performed and the output pulse from SOA showed frequency shift after filtration.

Similar device at 100 GB/s was used to make EXOR gate at wide wavelength range from 1540 nm to 1570 nm. The XGM in SOA, here showed that injected and modulated probe and pump signal change the carriers in active region to produce the gate. The excited charge carriers at high energy levels stimulated the emission of photons as amplified signal. The process is termed as gain saturation.

A SOA assisted Sagnac Interferometer switch has been used to make all optical XOR gate at 5 GHz and contrast ratio of 14.6 Db (Houbavlis et al., 1999). Polarization preserving passive components was used to cascade the SOA at 1000 m and 400 mA. The SOA had three optical signal inputs inclusive of a clock. The observation at the ports of reflection and transmission showed low switching energy of gate and high contrast ratio of ON-OFF states. This ratio depended on gain and recovery time of SOA and signal pulse widths. The best parameter for the gate here is the width of clock and the input pulse length. A NOT gate has been demonstrated using gain clamped SOA (GC-SOA) with small increase in laser power of approximately 2 dB (Stevan Jr & Teixeira, 2014). The SOA reached gain saturation and response time of latch principle showed similar results with extinction ratio of about 3.5 dB. The saturation effect of laser used showed that input power range increased from 0 to 2 dB for peak output power. The limitation experienced here showed that laser of 3 m fibre had a large resonant cavity and slow response time. This SOA gate operated at 1.244 GHz with improved extinction ratio of 5.5 dB. The modulation rate could be extended to maximize the NOT gate quality.

Demonstration of NOR gate has been done using FWM which is the property of SOA. This was done by checking its power levels at output for all possible values of input frequencies and optical power. The variables taken were active region length, injection current of SOA and the transmitters of input power. The three input signals at different frequencies are given as input to SOA which generate FWM for the logic function to be realized. The coupling of power pumps spreads the power of CW laser used. Filtration was done to remove unwanted signals and for low and high value of power to be obtained as logic 0 or 1.

Interferometric structure of Terahertz Optical Asymmetric Demultiplexer (TOAD) comprising of SOA demonstrated logic XOR gate (Wang, Wu, Shi, Yang & Wang, 2009). It exploited slow optical non-linearities presented in SOA and allowed controlled signal pulses distinguished by polarization or wavelength at switching energy of <1 pJ. The gain here and non-linear phase difference affected the output power XOR gate. Similar results for this gate were also demonstrated using SOA based MZI at 40 GB/s where two SOAs were used (Zhang, Zhao, Wang, Wang & Ye, 2003).

2.2 Theory of Optical Fibre

Optical fibre is a dielectric material usually made from glass, which is the core, and surrounded by layer of glass or plastic for cladding characterized by refractive index lower than that of the core. It is used as a waveguide for transmission of light under principle of total internal reflection in the core-cladding interfaces as shown in Fig 2.1.

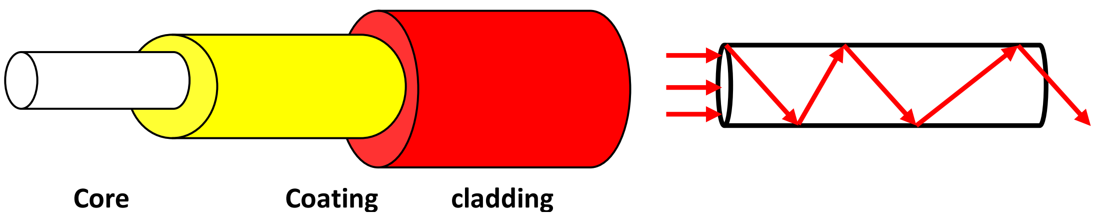

Fig. 2.2: Diagrammatic representation of optical fibre and light propagation within the core. (Agrawal 2012)

The optic fibres are more advantageous for use in data transmission since;

1. They have immense binary flow rates, of the order of several Tb/s, of which under laboratory conditions they reach the order of 10 Tb/s.
2. They have Low attenuation and therefore, the signal can be transmitted over long distances without regeneration;
3. Have bit error rate lower than 10^{-10}.
4. Have no inter-fibre crosstalk during signal propagation;
5. Do not create external electromagnetic field,

6. Resistant to external electromagnetic field perturbations

The disadvantages of using the optic fibre for transmission are;

1. Have higher initial cost than copper.
2. Likely to meltdown at higher optical powers.
3. Require expensive and difficult connections compared to those of copper media (Buck, 2004).

The Critical angle Θ_{cr} on light propagation within the core of the fibre is given by;

$$\Theta_{cr} = arcsin\left(\frac{n_{cl}}{n_{co}}\right) \dots \dots \dots \dots \dots \dots \dots \dots \dots \dots \dots \dots \dots \dots \dots (2.1)$$

The incident wave penetrates the medium which is less dense and results to phase shift between the incident and the reflected wave,

$$tg\,\frac{\phi}{2} = \left[\frac{sin^{\,2}(\Theta_{gr})}{sin^{\,2}\xi} - 1\right]^{\frac{1}{2}} \dots \dots \dots \dots \dots \dots \dots \dots \dots \dots \dots \dots \dots . \dots (2.2)$$

where, $\xi = \frac{\pi}{2} - \Theta$ is angle between optical fibre axis and wave vector of light propagating in waveguide. Light is propagated in fibre as single mode for normalized frequency given by

$$v = \frac{2\pi a}{\lambda_0}\sqrt{(\,n_1^2 - n_2^2\,)} \dots \dots \dots \dots \dots \dots \dots . \dots \dots \dots \dots \dots \dots \dots . \dots (2.3)$$

where a is diameter of fibre, λ_0 is wavelength of light propagating in fibre, n_1^2 *and* n_2^2 are refractive index for core and cladding respectively. During fibre rotation about optical axis, light undergoes phase change and the phase difference is given by,

$$\Delta\Phi = \Phi_0 - \Phi_e = \frac{2\pi v\,(n^0 - n^e)\,l}{c} \quad \ldots\ldots\ldots\ldots\ldots\ldots\ldots\ldots\ldots (2.4)$$

for plane wave, the electric field component **E** is;

$$E = E_0\, Cos\,(\omega t - kx) \quad \ldots\ldots\ldots\ldots\ldots\ldots\ldots\ldots\ldots\ldots\ldots\ldots\ldots (2.5a)$$

where,

$$k\chi = \phi = kl = \frac{2\pi\, l}{\lambda} = \frac{2\pi v\, l}{c} \quad \ldots\ldots\ldots\ldots\ldots\ldots\ldots\ldots\ldots\ldots\ldots (2.5b)$$

In Polarization Maintain Fibre (PMF), polarization doesn't change. The optical axis at an angle to polarization direction creates two orthogonal components i.e the slow and fast beams (birefringence), which generates the periodical change in the phase difference. For example, 45^o angle, results to linear polarization, followed by elliptical and circular polarization as shown in Fig 2.2.

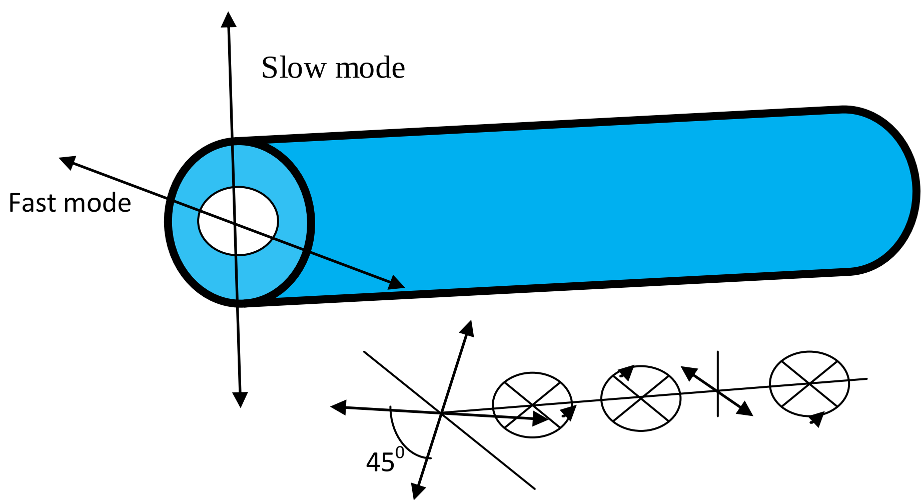

Fig. 2.3: Evolution of state of polarization along PMF for input signal polarized linear from slow axis at 45^0 (Barnoski, 2012)

The maintenance of polarization in optical fibres is by high or low birefringence. The measure of birefringence is defined by equations;

$$B_m = \frac{(B_y - B_x)}{K_0} = n_{ef}^{x} - n_{ef}^{y} \ldots\ldots\ldots\ldots\ldots\ldots\ldots\ldots\ldots\ldots\ldots\ldots\ldots\ldots\ldots \ldots (2.6)$$

$$L_B = \frac{2\pi}{|B_y - B_X|} \ldots\ldots\ldots\ldots\ldots\ldots\ldots\ldots\ldots\ldots\ldots\ldots\ldots\ldots\ldots\ldots\ldots\ldots\ldots\ldots\ldots (2.7)$$

where, B_y and B_x are propagation constants of orthogonal modes, n_{ef}^{x} and n_{ef}^{y} are effective refractive indexes, K_0 is wave vector and distance L_B is distance necessary for increase of orthogonal modes difference of $\frac{\pi}{2}$.

2.2.1. Propagation of light in optical fibres

The propagation of light is described by Maxwell equations under the assumption of nonlinear polarization, dielectric constant, ε since the loss in optical fibre is low in spectrum range of interest for fibre optics techniques and refractive index since it does not depend on core and cladding spatial coefficients, then the wave equation is in the form of Helmholtz equation,

$$\nabla^2 E + n^2(\omega) K_0^2 E = 0 \ldots\ldots\ldots\ldots\ldots\ldots\ldots\ldots\ldots\ldots\ldots\ldots\ldots\ldots\ldots\ldots (2.8)$$

Using polar coordinates (r,ϕ, z) in cylindrical symmetry of optical fibres, equation changes to,

$$\frac{\partial^2 E}{\partial r^2} + \frac{1}{r}\frac{\partial^2 E}{\partial r^2} + \frac{1}{r^2}\frac{\partial^2 E}{\partial r^2} + \frac{\partial^2 E}{\partial z^2} + n^2 K_2^2 E = 0 \ldots\ldots\ldots\ldots\ldots\ldots\ldots (2.9)$$

where,

$$E = R(r)\Phi(\phi)Z(z) \ldots\ldots\ldots\ldots\ldots\ldots\ldots\ldots\ldots\ldots\ldots\ldots\ldots\ldots\ldots\ldots\ldots\ldots (2.10)$$

The wave in fibre can be polarized under superposition of waves and by variable separation above equation can be solved as

$$\frac{1}{Z}\frac{d^2Z}{dz^2} = -\left(\frac{1}{R}\frac{d^2R}{dr^2} + \frac{1}{Rr}\frac{dR}{dr} + \frac{1}{r^2\Phi}\frac{d^2\Phi}{d\phi^2} + n^2K_0^2\right) \dots\dots\dots\dots\dots\dots\dots (2.11)$$

We can denote left hand side with constant γ^2 where, $\gamma = \alpha + i\beta$

Hence;

$$\frac{1}{z}\frac{d^2z}{dz^2} = \gamma^2 \dots\dots\dots\dots\dots\dots\dots\dots\dots\dots\dots\dots\dots\dots\dots\dots\dots\dots\dots\dots\dots\dots\dots\dots.. (2.12)$$

Solving it, then;

$$Z(z) = C_1\, e^{-\gamma z} + C_2\, e^{\gamma z} \dots\dots\dots\dots\dots\dots\dots\dots\dots\dots\dots\dots\dots\dots\dots\dots. (2.13)$$

This represents signals in opposite directions, along fibre axis where C_1 and C_2 are constants determined at the boundary conditions. At the boundary condition, $C_2 = 0$. Equation (2.11) changes to,

$$\frac{1}{Z}\frac{d^2Z}{dz^2} = -\left(\frac{r^2}{R}\frac{d^2R}{dr^2} + \frac{r}{R}\frac{dR}{dr} + r^2\gamma^2 + \gamma^2 n^2 K_0^2\right) \dots\dots\dots\dots\dots... (2.14)$$

Representing the left hand side with constant $-m^2$ and solving it we obtain;

$$\Phi(\phi) = C_3\cos(m\phi) + C_4\sin(m\phi) \dots\dots\dots\dots\dots\dots\dots\dots\dots\dots\dots.. (2.15)$$

where (ϕ) must meet condition of rotational symmetry $\boldsymbol{\Phi}(\phi) = \boldsymbol{\Phi}(\phi+2\pi)$, then m in equation (2.15) must be an integer. Substituting γ^2 and m^2 to equation (2.11) we obtain,

$$\frac{d^2R}{dr^2} + \frac{1}{r}\frac{dR}{dr} + \left(h^2 - \frac{m^2}{r^2}\right)R = 0.. \dots\dots\dots\dots\dots\dots\dots\dots\dots.. (2.16)$$

where,

$$h^2 = \gamma^2 + n^2K_0^2 \dots\dots\dots\dots\dots\dots\dots\dots\dots\dots\dots\dots\dots\dots\dots\dots\dots.. (2.17)$$

Solution for the ordinary differential equation (2.16) for the conditions h = h_1 for r < a (core) and h>ih_2 for r>a (cladding) forms the Bessel's function,

$$R(r) = C_5 J_m(h_1 r) + C_6 N_m(h_1 r). \ldots \ldots \ldots \ldots \ldots \ldots \ldots \ldots \ldots \ldots \ldots \ldots . (2.18)$$

Function J_m is Bessels function of first kind and N_m is Bessel function of second kind and m order and is called Neumman function. Assuming that C_6= 0 and substituting equations (2.18) , (2.15) , (2.13) to Equation (2.10) results to,

$$E_z = J_m(h_1 r)(A_1 \mathrm{Cos} m\phi + B_1 \mathrm{Sin}\, m\phi)e^{-\gamma z} \ldots \ldots \ldots \ldots \ldots \ldots \ldots \ldots \ldots (2.19)$$

and equation (2.16) can be solved,

$$R(r) = C_7 I_m(h_2 r) + C_8 K_m(h_2 r) \ldots \ldots \ldots \ldots \ldots \ldots . \ldots . . \ldots \ldots \ldots \ldots (2.20)$$

I_m is modified Bessel function of first kind, K_m is modified Bessel function of second kind and m^{th} order. Assuming C_7 = 0 and further substitution, Equation 2.10 changes to,

$$E_z = K_m(h_2 r)(A_2 \mathrm{Cos} m\phi + B_2 \mathrm{Sin}\, m\phi)\, e^{-\gamma z} \ldots \ldots \ldots \ldots \ldots \ldots \ldots \ldots (2.21)$$

This is for r > a. The magnetic field intensity vector H can be solved the same way and

$$H_z = J_m(h_1 r)(F_1 \mathrm{Cos} m\phi + G_1 \mathrm{Sin}\, m\phi)e^{-\gamma z} \ldots \ldots \ldots \ldots \ldots \ldots \ldots \ldots . . (2.22)$$

$$H_z = K_m(h_2 r)(F_2 \mathrm{Cos} m\phi + G_2 \mathrm{Sin}\, m\phi)e^{-\gamma z} \ldots \ldots \ldots . . \ldots \ldots \ldots \ldots . (2.23)$$

Where F_1, F_2, G_1, G_2 are constants which can be determined from boundary conditions (Ientilucci,1993), (Agrawal, 2001).

2.2.2. Fibre dispersion

The fibre has attractive aspects mentioned in section 2.2 in optical communication networks. The major one being its enormous bandwidth. However, its challenge is on dispersion and nonlinearity. In single mode fibre, source of dispersion is group velocity dispersion (GVD), where wavelength depends on group velocity, Vg. This results to spectra of different group velocities. For fibre of length z, the spectral component of frequency ω exits the fibre at time delay T given by;

$$T = \frac{Z}{v_g} \quad \ldots\ldots\ldots\ldots\ldots\ldots\ldots\ldots\ldots\ldots\ldots\ldots (2.24)$$

where, $v_g = \frac{d\omega}{d\beta}$, β is phase (propagation) constant. The pulse having the spectral width , $\Delta\omega$ is broadened by,

$$\Delta T = \beta_2 Z \Delta\omega \ \ldots\ldots\ldots\ldots\ldots\ldots\ldots\ldots\ldots\ldots\ldots\ldots (2.25)$$

where, $\beta_2 = \frac{d^2\beta}{d\omega^2}$ which is the GVD parameter. Since in optical fibre communication systems wavelength is used more often than frequency unit, equation (2.25) changes to;

$$\Delta T = DZ\Delta\lambda \ldots\ldots\ldots\ldots\ldots\ldots\ldots\ldots\ldots\ldots\ldots\ldots\ldots (2.26)$$

where, Δλ is signal spectral width in wavelength units. D is dispersion parameter related to β_2 by,

$$D = \frac{d}{d\lambda}\left[\frac{1}{v_g}\right] = -\left(\frac{2\pi c}{\lambda^2}\right)\beta_2 \ldots\ldots\ldots\ldots\ldots\ldots\ldots\ldots\ldots (2.27)$$

where, c is velocity of light in vacuum. When fibre loss and nonlinearity are neglected, optical fibre causes wave distortion and optical fibre is considered as all-pass filter with non linear phase response and the transfer function is;

$$H_0(\omega) = exp\{jz\,[\beta_0 + \beta_1(\Delta\omega) + \frac{1}{2}\beta_2(\Delta\omega)^2 + \frac{1}{6}\beta_3(\Delta\omega)^2 + \ ...]\}\ (2.28)$$

where, $\beta_m = \left(\frac{d^m\beta}{d\omega^m}\right)_{\omega=\omega_0}$, ω_0 is operating frequency and m =0,1,2,...

The first term of this equation causes constant phase shift, second term is for time delay while other terms are source of dispersion. The third term is related to dispersion slope S given by;

$$S = \frac{dD}{d\lambda} = \left(\frac{2\pi c}{\lambda^2}\right)^2 \beta_3 + \left(\frac{4\pi c}{\lambda^3}\right) \beta_3 \ \ldots\ldots\ldots.\ldots\ldots\ldots\ldots\ldots\ldots..(2.29)$$

2.3 Theory of SOA

Semiconductor Optical Amplifier is an optoelectronic component characterized by a unidirectional or bidirectional access and it works due to electrical current injection, spontaneous and stimulated emission. It is manufactured using alloys such as gallium arsenide (GaAs) or Indium Phosphide (InP). The basic advantages of the SOA are (Said, Rezig & Bouallegue, 2010);

1. Polarization dependent – require polarization maintaining fibre.
2. Relatively high gain of approximately upto 20 dB.
3. Output saturation power ranges from 5 to 10 dBm.

4. Can operate at 800, 1300, and 1500 nm wavelength regions i.e wide bandwidth.
5. Compact and easily integrated with other devices.
6. Can be integrated into arrays for multichannel operations.
7. High noise and cross-talk levels due to nonlinear phenomenon such as FWM.
8. Amplification occurs primarily through the stimulated emission process.
9. The medium is pumped until a population inversion state is achieved. Pump powers are typically between 20 to 250 mW. An isolator is used to reduce reflections at the input to the amplifier while a narrow band optical filter is used to reduce transmission of amplified spontaneous emission frequency components.
10. The resultant optical gain depends both on the optical frequency and the local beam intensity within the amplifier section i.e.it is transparent (Hong, Spencer, & Shore, 2004).

SOA is used for all-optical signal processing tasks at very high bit rates that cannot be handled by electronics, such as in wavelength conversion, signal regeneration, optical switching as well as logic operations. It uses non-linear effects; FWM, XGM, SPM though they suffer low conversion efficiency, high input power and depend on polarization. All-Optical gates are made from this device because of their increasing advantages on performance of computing machines and especially towards optical communication network (Sarkar & Mukhopadhyay). Flip flops and latch devices have been developed using SOA, though challenges still exist but great importance is that it has been utilized to boost speed in optical networks in communication.

2.3.1 Working of SOA

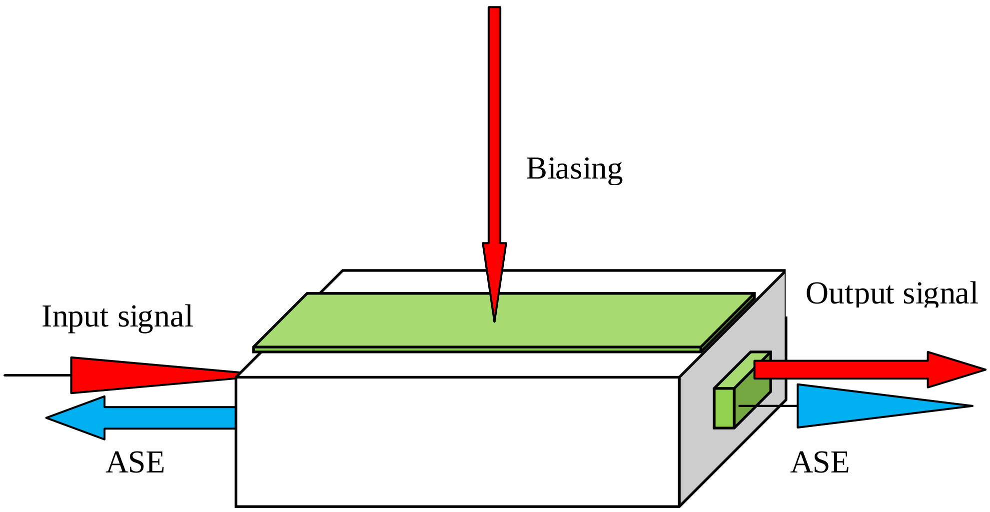

Fig. 2.4: The structure of the WTW SOA (Said & Rezig, 2011).

When signal is injected to the SOA as shown in Fig 2.3, there is modulation of gain, caused by change in refractive index and carrier density in the active region. This brings change in phase, frequency and amplitudes which result to wavelength conversion witnessed by XPM, XGM or in FWM (Connelly, 2001). Input signal is required for inverted modulation accompanied by chirp and low extinction ratio. Low signal power is required for XPM and the output is of high quality. Modulation in FWM is independent and is sensitive to polarization and frequency whereas dispersion is resolved due high speed the SOA.

2.3.2 Wavelength converter

Wavelength conversions occur when data arriving on one wavelength link is changed to another wavelength along another link and the technique used can be optical-electrical (O/E) or all optical (Kleinberg & Kumar, 2001). O/E uses a photodectector for their translations which makes it disadvantageous since it's more complex and consumes more power. Some data could be lost in the process due to phase frequency or analogue amplitude change. On the contrary, all-optical is preferred since the signal remains in optical domain continuously to the receiver (Liu et al, 2007). The wavelength converter has the following special characteristics.

1. They are transparent to bit rates and signal formats.
2. They have the ability to convert long and short wavelengths signals.
3. They can moderate the input power.
4. Insensitive to input signal polarization and possess.
5. Low chirp output.
6. They are simple in implementing.
7. They are easy to convert all range wavelengths.

2.4 Noise effects in SOA.

Noise is generated in SOA due to Amplified spontaneous emission (ASE) and do interact nonlinearly with injected signal to produce other Noise;

1. Shot noise.
2. Signal spontaneous beat noise.
3. Spontaneous –spontaneous beta noise.

Noise determines the Bit Error Rate (BER) of the system transmission. The power of ASE noise generated internally within the SOA is given by,

$$P_{ASE} = 2.n_{sp}.h.v.(G-1).B_o \dots\dots\dots\dots (2.30)$$

where G, is the gain at the optical frequency v, h represents the Planck's constant, B_0 is the optical bandwidth of a filter within which P_{ASE} is determined, n_{sp} is the population inversion factor also known as spontaneous emission factor. For an ideal amplifier, $n_{sp}=1$ and results to complete inversion, if $n_{sp}>1$ population inversion is partial. Total optical power can be detected due to signal and the power of ASE noise which results to shot noise (N_{shot}) and is given by;

$$N_{shot} = 2.e^2.B_e\left[\frac{G.P_{in}}{h.v} + n_{sp}.B_o.(G-1)\right] \dots\dots\dots\dots (2.31)$$

where B_e is the electrical bandwidth of the photo-detector. Shot noise power is related to signal power and ASE of the frequency. This is comparable to signal – spontaneous beat noise (N_{s-sp}) which occurs between optical signals and ASE frequencies closer to those of optical signals and is given by;

$$N_{s-sp} = 4.\frac{e^2}{h.v}.B_e.P_{in}.n_{sp}.G(G-1) \dots\dots\dots\dots (2.32)$$

The spontaneous-spontaneous beat noise (N_{sp-sp}), which occurs between ASEs, is expressed as;

$$N_{sp-sp} = e^2(2.B_0 - B_e).B_e.n_{sp}^2.(G-1)^2 \dots\dots\dots\dots (2.33)$$

Its worth to note here that, N_{sp-sp} can be minimized using a filter of bandwith B_o after the amplifier. N_{s-sp} dominates only at strong input signal while N_{sp-sp} is at injection input power. These noises can be summed up using Noise Figure (NF) parameter which is due to amplification process of SOA. NF is the ratio of optical signal to noise ratio (OSNR) of the signal at input and output of the SOA (Baveja, Maywar & Agrawal, 2012).

$$\mathrm{NF} = \frac{\mathrm{OSNR_{in}}}{\mathrm{OSNR_{out}}} \ldots\ldots\ldots\ldots\ldots\ldots\ldots\ldots\ldots\ldots\ldots\ldots\ldots\ldots\ldots\ldots\ldots\ldots\ldots (2.34)$$

where,

$$\mathrm{OSNR_{in}} = \frac{\mathrm{P_{in}}}{2\mathrm{hvB_e}} \ldots\ldots\ldots\ldots\ldots\ldots\ldots\ldots\ldots\ldots\ldots\ldots\ldots\ldots\ldots\ldots\ldots (2.35)$$

$$\mathrm{OSNR_{out}} = \frac{\mathrm{e.P_{in}\,G}}{\mathrm{hv}} \cdot \frac{1}{\mathrm{N_{shot}} + \mathrm{N_{s-sp}} + \mathrm{N_{sp-sp}}} \ldots\ldots\ldots\ldots\ldots\ldots\ldots (2.36)$$

substituting equations (2.31), (2.35) and (2.36) to (2.34), then,

$$\mathrm{NF} = \frac{1}{\mathrm{G}} + 2.\mathrm{n_{sp}}.\frac{\mathrm{G}-1}{\mathrm{G}} + \frac{\mathrm{h.v.B_o.n_{sp}.P_{in}.(G-1)}}{\mathrm{P_{out}^2}} + \frac{\mathrm{h.v(2B_o - B_e).n_{sp}^2.P_{in}.(G-1)^2}}{2\mathrm{P_{out}^2}} \ldots\ldots\ldots\ldots\ldots (2.37)$$

For weak ASE with respect to input power, and neglecting the last two terms, equation (2.37) will be;

$$\mathrm{NF} \cong \frac{1}{\mathrm{G}} + 2.\mathrm{n_{sp}}.\frac{\mathrm{G}-1}{\mathrm{G}} \ldots\ldots\ldots\ldots\ldots\ldots\ldots\ldots\ldots\ldots\ldots\ldots\ldots\ldots (2.38)$$

From equation (2.38), NF= 3 dBm when G>>1, and n_{sp}=1, which gives the lowest value for an ideal amplifier. This implies that every time an optical signal is amplified, the signal to noise ratio is reduced to half. We can express equation (2.38) as a function of power as;

$$NF \cong \frac{1}{G} + 2.\frac{P_{ASE}}{h.v.G.B_o} \dots\dots\dots\dots\dots\dots\dots\dots\dots\dots\dots\dots\dots (2.39)$$

This equation is very significant because it allows us to choose the characteristics of the SOA in order to obtain the highest value of the G for a minimum NF. The highest value of NF can then be obtained for corresponding lowest value of gain. If the gain G is maximum satisfying criterion for low noise, then it is possible to choose the highest biased current possible for the SOA.

2.5 SOA amplification

Semiconductor Optical Amplifier (SOA) amplifies input light through stimulated emission by an electrical pump to achieve population inversion. Amplification in SOA depends on injected current, length of SOA, wavelength and levels of input power. Any input power results into decrease in gain saturation, depletion of carrier density and stimulated emission **Error! Reference source not found.**. This ffects the non-linearity properties of the SOA. The saturation output power (P_{Sat}) is given by;

$$P_{Sat} = \frac{A}{\Gamma} . I_s \dots\dots\dots\dots\dots\dots\dots\dots\dots\dots\dots\dots\dots\dots\dots\dots\dots\dots\dots (2.40)$$

Where, $I_s = \frac{h.v}{a_N \tau_s}$ and A is the cross sectional area of the active region, Γ is the coefficient of optical confinement factor, a_N is the differential modal gain and

τ_s makes references to the spontaneous carrier life time , I_s is the saturation input intensity.

From equation (2.40), high saturation output power is attained when bias current is high, which is inversely proportional to carrier density. This is an essential characteristic for SOA non- linearity particularly power boosters and other multichannel applications used in optical communication networks such as WDM, optical switches, wavelength converters, power equalizers, 3R regeneration and logic operations.

2.6 Four-Wave Mixing (FWM)

This is the nonlinear effect, where more than one wave present in the fibre for propagation are combined. The waves interact to generate another wave whose intensity is proportional to intensities of interacting ones known as idler as shown in the Fig. 2.4. The probe or signal light originally present, sandwich the pump with the Idler light for the two channels. The phase of the wave and information is preserved and multiple waves can be mixed to generate signal with different frequencies. FWM offers strict transparency in modulation and bit rate, though it has low conversion efficiency, power depletion and crosstalk, it needs high care on control of polarization. It is ultrafast and capable of multi-wavelength conversations. It's more advantageous since it has the affinity to work at high GB/s. Though, this interaction has low efficiency, and levels of noise in signal are minimal its a suitable method for the generation of the all optical gates in the essence that the signals are coupled together to produce logic gate from the SOA (Hedekvist, Bhardwaj, Vahala & Andersson, 2001). For example, the FWM will generate OR gate only when either inputs are low or high, while for the AND gate, both inputs are high. This works only at different input signals frequency coupled together through the fibres and in the SOA where FWM occur.

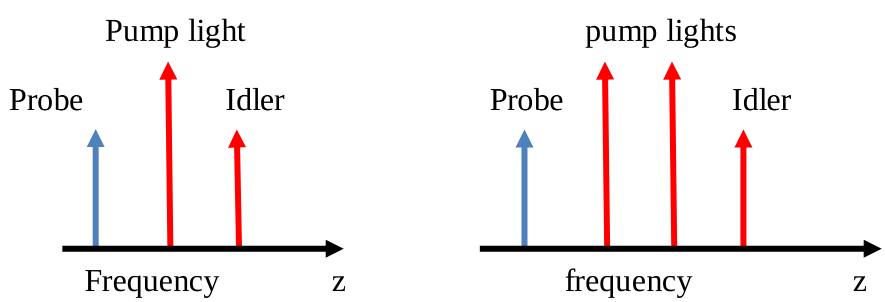

Fig. 2.5: Four wave mixing for pump waves. (Saxena, 2015).

For two signals;

$$w_{ij} = w_i - w_j \quad \ldots\ldots \quad (2.41)$$

For three signals;

$$w_{ijk} = w_i + w_j - w_k \quad \ldots\ldots \quad (2.42)$$

The input signals give out their energies by interaction to form new frequencies w_{ij} and w_{ijk}. The generated signal for N interacting signals is,

$$M = \frac{N^2(N-1)}{2} \quad \ldots\ldots \quad (2.43)$$

The power for the new frequency w_{ijk} is proportional to the FWM efficiency given by,

$$\eta = \frac{\alpha^2}{\alpha^2 + \Delta\beta^2}\left(1 + \frac{4e^{-\alpha z}\, sin^2\, \frac{\Delta\beta z}{2}}{(1 - e^{-\alpha z})^2}\right) \ldots \ldots \ldots \ldots \ldots \ldots \ldots \ldots \ldots . \ldots . . (2.44)$$

where α is the attenuation coefficient, $\Delta\beta$ is the phase mismatch that represents the difference of propagation constants β of the original signals and the FWM-generated signals and η is FWM efficiency.

2.7 Self Gain Modulation (SGM)

This is the Modulation of gain induced by variation of input signal power. It can be used to conceive the compensator of the distortion of the signal in the WTW SOA.

2.8 Self Phase Modulation (SPM)

This is the modulation of phase of WTW SOA output signal caused by refractive index variation due to change of input power. SPM results in the conversion of variations of optical intensity to phase. The refractive index n of an optical fibre is given by;

$$n = n_0 + n_2 I\ (\tau) \ldots \ldots \ldots \ldots \ldots \ldots \ldots \ldots \ldots \ldots \ldots \ldots \ldots \ldots \ldots \ldots \ldots \ldots \ldots (2.45)$$

where n_0 is the linear refractive index of the material approximated to be 1.5, n_2 is the non linear refractive index and is equal to $3x10^{-20}\ m^2/W$ and $I(\tau)$ is the optical intensity in units of W/m^2. The value of n_2 may be small but high signal intensity along transmission distance make the effect of nonlinear refractive index not negligible. For example, for a propagation distance of *z,* the phase of the signal is given by,

$$\Phi(z,\tau) = \frac{2\pi}{\lambda}\ n_0 z\ + \frac{2\pi}{\lambda}\ n_2 I(z) z_{eff}\ \dots\dots\dots\dots\dots\dots\dots..\dots\dots\dots\dots\dots\ (2.46)$$

where *Zeff* is the effective transmission distance taking into account of the fibre attenuation. The first term is linear phase shift and depends on transmission distance z, whereas, the second term depends on distance and intensity variation of the signal. When $Z_{eff} < z$, then the fibre attenuation reduces the effect of nonlinear phase shift. SPM broadens the signal spectrum and it doesn't affect the intensity of the signal. The spectral broadening effect arise from the fact that the time-dependent phase variation causes instantaneous frequency deviation **δω (τ),** which is given by,

$$\delta\,\omega(\tau) = -\ \frac{\delta\phi}{\delta\tau}\ = -\frac{2\pi}{\lambda}\,n_2\,z_{eff}\ \frac{\delta I(\tau)}{\delta\tau}\ \dots\dots\dots\dots..\dots\dots\dots\dots\ (2.47)$$

This equation suggests that the magnitude of instantaneous frequency deviation increases with distance and the intensity variation of the signal. The broadening of the spectrum may result to crosstalk between the channels in WDM systems. The combined effect of dispersion and SPM strongly depends on the sign of dispersion (D), hence SPM have no effect on intensity of the signal. SPM enhances the effect of dispersion when the operating wavelength is in the normal dispersion regime. This results from the fact that the sign of instantaneous frequency variation across the pulse induced by the SPM is identical to that induced by the dispersion. Equally, for a strong SPM, a pulse is compressed during initial propagation. In addition, under ideal conditions the pulse shape can be continually preserved during propagation due to the balancing of the effects of dispersion. However, the effect of SPM decreases with transmission distance due to fibre attenuation.

2.9 Cross Gain Modulation (XGM)

This is similar to SGM. It is the modulation of the induced gain by the optical signal i.e pumps or control signal affecting the gain of probe signal. Its co-propagative and counter propagative configuration in the SOA.

2.10 Cross Phase Modulation

This is similar to the SPM and it corresponds to the change of refractive index induced by the control pump or signal affecting phase of other optical signal (probe) which propagate simultaneously in the SOA. However, in this case the total nonlinear phase shift on a given channel is due to the combined intensities of all transmitted channels, which can result in cross talk among WDM channels. When *N* channels are transmitted in a single optical fibre, the nonlinear phase shift on the j th channel is governed by,

$$\Phi_j(z,\tau) = \frac{2\pi}{\lambda}\ n_0 z\ + \frac{2\pi}{\lambda}\, n_2 I(z) z_{eff}\ \left[I_j(\tau) +\ 2\sum_{m\neq j}^{N} I_m(\tau)\right] \ldots\ldots\ldots (2.48)$$

where $I_m(\tau)$ is the optical intensity of the m *th* channel, $I_j(\tau)$ corresponds to SPM whereas the second term in parenthesis is responsible for XPM. The factor of 2 suggests that the effect of XPM to that of SPM from a neighboring channel is two times stronger. However, the effect of XPM depends on the relative temporal locations of pulses when considered at different wavelengths. XPM is also strong when pulses completely overlap one another. The effect of XPM is reduced when all channels transmit at 1 bit. Large dispersion discrepancies among channels results to rapid pulses walk off from one another. In other words, the effect of XPM is inversely proportional to dispersion discrepancies among channels in WDM systems. Here, chromatic dispersion plays a key role in modulation of gain of signal due to saturation. The phase of the signal is affected by fluctuations intensity of signal power of one channel. To minimize the impairment caused by XPM, the channel separation and/or local dispersion have to be properly chosen in WDM systems, which can be achieved in practice.

2.11 Self Induced Nonlinear Polarization Rotation

This translates the self rotation of the polarization state of the SOA output signal with respect to input signal.

2.12 Cross Polarization Modulation (XpolM)

This is similar to SPR and occurs due to polarization rotation of a beam in the SOA under influence of polarization and power of relatively strong pump (Guo & Connelly, 2005). The new birefringence and gain compression affects the SOA by producing different phase and gain compressions of gain saturation difference of transverse electric (TE) and Transverse magnetic (TM). This results to the rotation of the polarization state of each signal. The magnitude of this is affected by bias current and input signal power of WTW SOA.

These nonlinearities can be used in All Optical Gates required in wavelength routing in high speed Optical time domain multiplexing (OTDM) networks (Berrettini, Simi, Malacarne, Bogoni, & Poti, 2006), (Teimoori et al, 2008).

2.13 Polarization rotation using stokes parameters.

Stoke parameters describe polarization states change of electromagnetic wave in SOA at the output with respect to input for various lengths of active region (Acosta, Maldonado, & Soto, 2008). Defined as;

$$\begin{pmatrix} S_O \\ S_1 \\ S_2 \\ S_3 \end{pmatrix} = \begin{pmatrix} A_{TE}^2 + A_{TM}^2 \\ A_{TE}^2 - A_{TM}^2 \\ 2.A_{TE}.A_{TM}.Cos\,(\phi_{TM} - \phi_{TE}) \\ 2.A_{TE}.A_{TM}.Sin\,(\phi_{TM} - \phi_{TE}) \end{pmatrix} \ldots\ldots\ldots\ldots\ldots (2.49)$$

where So is the parameter that translates the total intensity, S_1 refers to intensity difference between horizontal and vertical polarization,S_2 refers to difference between intensities transmitted by the axes (45°, 135°),S_3 is a parameter that expresses the difference between intensities transmitted for the left and right circular polarizations and denote the phase shift for the TE and TM modes, respectively. At the output of the SOA, the normalized stoke parameters is given by;

$$S_i = \frac{S_i}{S_o} \quad ; i = (\ 1\ ,2,3\ ) \ldots\ldots\ldots\ldots\ldots\ldots\ldots\ldots\ldots (2.50)$$

whereas the phase shift variation is,

$$\Delta\phi = \phi_{TM} - \phi_{TE} = arctan\left(\frac{S_3}{S_2}\right) \ldots\ldots\ldots\ldots\ldots\ldots\ldots (2.51)$$

while for orientation azimuth ψ and ellipticity χ angles are;

$$\begin{pmatrix} S_1 \\ S_2 \\ S_3 \end{pmatrix} = \begin{pmatrix} \cos(2\psi).\cos(2\chi) \\ \sin(2\psi).\cos(2\chi) \\ \sin(2\chi) \end{pmatrix} \ldots\ldots\ldots\ldots\ldots\ldots\ldots (2.52)$$

Polarization change at output of SOA then is;

$$\begin{cases} \psi = \frac{1}{2}\arcsin\left(\frac{s_2}{s_1}\right) \\ \chi = \frac{1}{2}\arcsin S_3 \end{cases} \ldots\ldots\ldots\ldots\ldots\ldots\ldots (2.53)$$

2.14 Gain in the SOA

Optical signals coupled in saturated SOA along amplifier length (z direction) are decomposed in the TE and TM component and the gain coefficients are not constant and are written as;

$$\begin{cases} g_{TE}(z) = \Gamma_{TE}\,.\;g_m(z).\alpha_{TE} \\ g_{TM}(z) = \Gamma_{TM}\,.g_m(z)\alpha_{TM} \end{cases} \ldots\ldots\ldots\ldots\ldots\ldots\ldots (2.54)$$

where g_{TE} and g_{TM} are the gain coefficients, Γ_{TE} and Γ_{TM} denote the confinement factors, α_{TE} and α_{TM} symbolize the efficient losses, respectively for TE and TM modes. g_m designates the material gain coefficient. The polarization sensitivity of a saturated amplifier can be estimated by assuming the material intensity gain coefficient to be saturated by the light intensity and the gain of material, $g_m(z)$ will be given by;

$$g_m(z) = \frac{g_{\,m,o}}{(1 + (|A_{TE}(z)|^2 + |A_{TM}(z)|^2).E_s^{-2})} \ldots\ldots\ldots (2.55)$$

2.15 Theory on logic gate

This is a basic electronic block having one or more than one input to give one output. The relationship between the input and the output is based on logic operations of the gate. In electronics, they are implemented using diodes or transistors which act as switches. The gates are NOT, AND, NAND, OR, NOR and EXNOR. Logic circuits that use these gates are multiplexers, registers, Arithmetic Logic Units (ALU), computer memory or even microprocessors. These gates however, have been replaced by the programmable logic devices which use a number of logic gates to form a single integrated circuit (IC). The IC is much faster, smaller and consumes less power. It also allows feedback between its input and output (cascading) though its results to propagation delay due to change over. The electronics can't fit to operate here, at high frequencies or bandwidths hence the need to replace them by Optical domain. Data transport then has been in optical domain due to the speed up of change over of optical communication networks which need photonics crystals or optical integrations for compatibility. All optical signal processing has been utilized for this purpose since non linearity materials are required for their strength. The advantages that these device have though are mentioned in chapter one, can be advanced that they operate at the powers of only few milliwatts which shows compatibility in telecommunication. These all-optical logical gates are based on interferometric designs, where the signal is split into two waveguide branches within a network (Kang et al, 2002, Manning, Giller, Yang, Webb & Cotter 2007). At one arm there is delay in signal and at the output they are made to interfere for certain behavior to be observed. For example, constructive interference could be ON, destructive could be OFF, and by stimuli variation, an all-optical gate is obtained due to change in refractive indices via controlled beams launched as inputs to get their outputs.

If we consider for example a two channel highly non linear optical material, with signal in z-direction, coupling is achieved from channel 1 to channel 2 and is given by coupled mode equations (Teich & Saleh, 1991, Saleh, Teich & Saleh, 1991).

$$\frac{da_1}{dz} = \int k_{21} e^{f\Delta\beta z} \; a_2(z) \ldots\ldots\ldots\ldots\ldots\ldots\ldots\ldots \quad (2.56)$$

$$\frac{da_2}{dz} = -\int k_{12} e^{-f\Delta\beta z} \; a_1(z) \ldots\ldots\ldots\ldots\ldots\ldots\ldots \quad (2.57)$$

where,

$$\Delta\beta = \beta_1 - \beta_2 \ldots\ldots\ldots\ldots\ldots\ldots\ldots\ldots\ldots\ldots \quad (2.58)$$

and

$$\kappa_{21} = \frac{1}{2}\,(n_2^2 - n^2)\frac{\kappa_0^2}{\beta_1^2}\int_a^{a+d} u_1\,(y) u_2\,(y) dy \ldots\ldots\ldots\ldots \quad (2.59)$$

$$\kappa_{12} = \frac{1}{2}\,(n_1^2 - n^2)\,\frac{\kappa_0^2}{\beta_2^2}\int_{-a-d}^{-a} u_2\,(y)\,u_1\,(y) dy \ldots\ldots\ldots\ldots \quad (2.60)$$

where u_1 and u_2 are the transverse mode distributions supported by channels one and two, respectively, and $\beta_{1,2}$ represents the propagation constants of the modes. At the boundary conditions where $a_1(0) = 1$ and $a_2(0) = 0$, coupled mode equations (2.56) and (2.57) are solved to become;

$$a_{1(z)=}a_1(0)e^{-\frac{f\Delta\beta z}{2}\left(cos\ (\Upsilon z)-f\ \frac{\Delta\beta}{2\Upsilon}\sin(\Upsilon z\ )\right)} \ldots\ldots\ldots\ldots\ldots.\ldots\ldots\ldots.(2.61)$$

$$a_{2(z)=}a_1(0)\frac{k_{12}}{j\Upsilon}e^{\left(-\frac{f\ \Delta\beta z}{2}\right)\sin(\Upsilon z\ )} \ldots\ldots..\ldots\ldots\ldots\ldots\ldots\ldots\ldots\ldots.(2.62)$$

$$\text{where,}\Upsilon^2 = \left(\frac{\Delta\beta}{2}\right)^2 + \kappa^2 \text{ and } \kappa = \sqrt{\kappa_{12}\ \kappa_{21}}$$

The optical power in each waveguide is proportional to the square of the field and is therefore given by;

$$P_1(z) = P_1(0)\left[cos^2(\Upsilon z) + \left(\frac{\Delta\beta}{2\Upsilon}\right)^2 sin^2(\Upsilon z)\right] \ldots\ldots\ldots\ldots\ldots\ldots.(2.63)$$

$$P_2(z) = P_1(0)\frac{|\kappa_{12}|^2}{\Upsilon^2}sin^2(\Upsilon z) \ldots\ldots\ldots\ldots\ldots\ldots\ldots\ldots\ldots\ldots\ldots.\ldots....(2.64)$$

During phase match, perfect coupling is achieved at Δβ=0, the equations simplify to;

$$P_1(z) = P_1(0)[cos^2(\kappa z)] \ldots\ldots\ldots\ldots..\ldots\ldots\ldots\ldots\ldots\ldots\ldots\ldots\ldots.\ldots.(2.65)$$

$$P_2(z) = P_1(0)sin^2(\kappa z) \ldots\ldots\ldots\ldots\ldots\ldots\ldots\ldots\ldots\ldots\ldots\ldots.\ldots\ldots\ldots\ldots(2.66)$$

And the power transfer ratio is expressed as;

$$R_p = \frac{P_2}{P_1} = \left(\frac{\pi}{2}\right)^2 sin\ c^2\left(\frac{1}{2}\sqrt{\left[1+\left(\frac{\Delta\beta L_c}{\pi}\right)^2\right]}\right) \ldots\ldots\ldots\ldots\ldots....(2.67)$$

All gates use the Kerr effect. Kerr effect is the change of refractive index of a medium that is directly proportional to square of optical field residing in the medium and is given by;

$$\eta = \eta_L\ \left(\ 1 + \frac{\eta_2\ |E|2}{Z_0}\ \right)^2 \ldots\ldots\ldots\ldots\ldots\ldots.\ldots\ldots\ldots\ldots\ldots\ldots\ldots\ldots.(2.68)$$

where η is a factor with respect to material characteristics and results to phase mismatch.

CHAPTER THREE

METHODOLOGY

3.1 Introduction

The approach employed in this study is discussed here, where Optisystem software version 7.0 was used to test and simulate the model setups for NOT-, AND- and OR- gates. The Optisystem Software v.7.0 is a modern designing tool for optical communication systems. The software was employed because it's non-online software hence portable.

3.2 Simulation set up

The setup shown in Fig.3.1 was theoretically constructed using several components to come up with the optical gates.

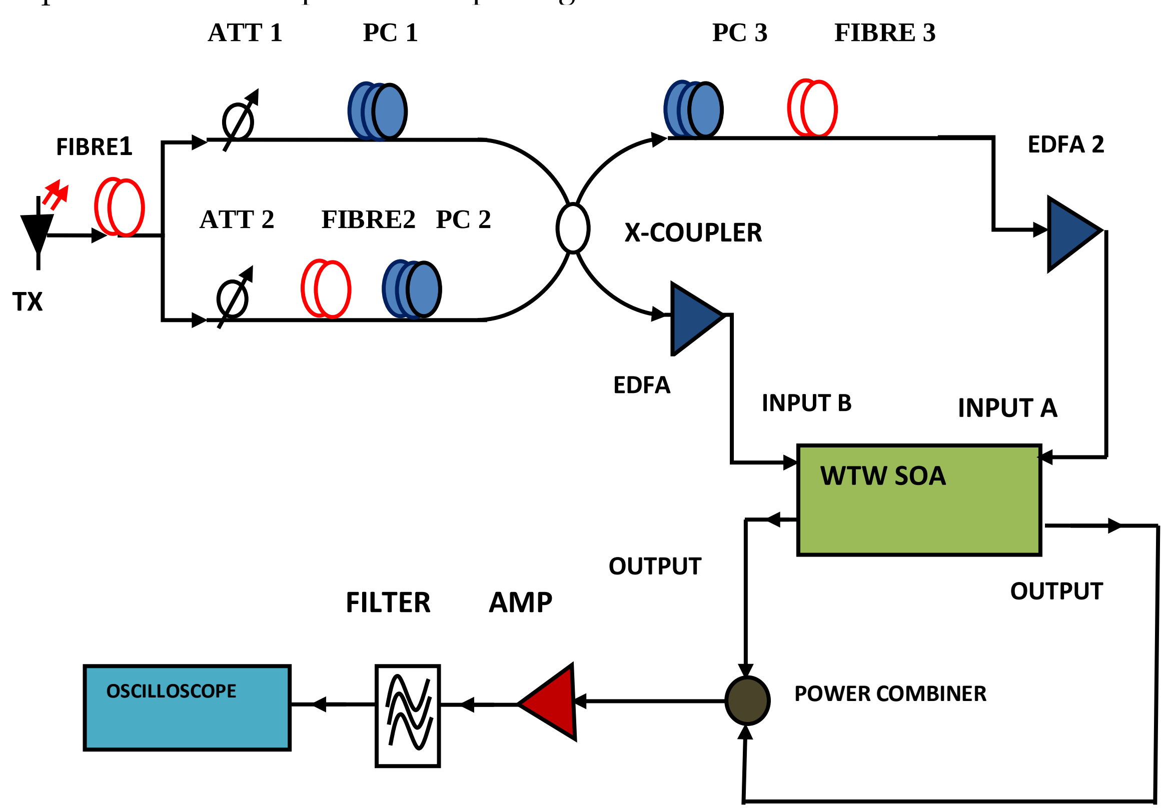

Fig 3. 1: General set up for the logic gates

A modulated signal pattern from transmitter was generated and injected through optical fibre 1. The signal was split into two channels; one signal through the Attenuator (ATT1), Polarization Combiner (PC1) and the other channel 2 signal through an Optical fibre2 and PC2. The ATT and PC were adjusted to obtain the average power and states of polarization (SOPs) of the signal and the pump respectively. On coupling of the signals, PC3 and fibre3 of specific length were used, amplification was done using EDFA1 and EDFA2 for the OR gate inputs. An Isolator replaced the EDFA2 for the AND gate since the average input power supply for the signal was sufficient. This was to maintain the signal in one direction thus protecting the signal channel from the counter-propagating the signal. ATT2, PC2 and EDFA1 were also not employed in the set up for the AND gate. The lengths of Fibre1, 2, 3 were varied for all the gates to obtain signal synchronization and overlap before injection to the WTW SOA as input A and input B. The lengths and injection currents for the WTW SOA were varied. The output signals were amplified, filtered and visualized using optical oscilloscope where they were analyzed and interpreted as discussed in chapter four.

CHAPTER FOUR

RESULTS AND DISCUSSIONS

4.1 Introduction

This chapter discusses the results obtained after several simulations using the Optisystem software and the input and output signals were analyzed using Origin software and interpreted. Initially, the research was carried out to establish whether WTW SOA can work as a switch and subsequently the optical gate switches.

4.2 SOA as a switch

To obtain the switching characteristics of WTW SOA, simulation set up in Fig 4.1 was used, where an input probe signal from transmitter (TX) at frequency of 1554 nm, having power of 5 dBm was multiplexed with a 0 dBm Continuous Wave (CW) pump signal at frequency of 1550 nm and launched into WTW SOA. At different lengths, the injection current of the WTW SOA was varied from a lower range of 0.1 to 0.5 A. The output power was measured using the optical power meter against the injection current for the selected lengths. The signals was studied using the optical oscilloscope as shown in Fig 4.1

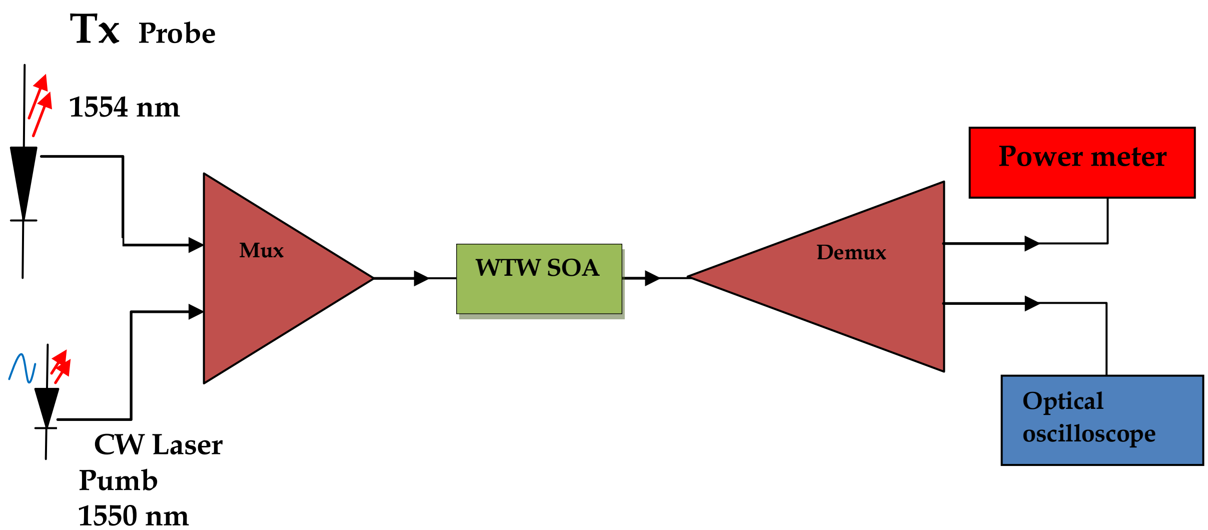

Fig. 4.1: Set up of WTW SOA as a switch.

Fig 4.2 shows the results at different switching currents points for different lengths when CW of 0 dBm was used to pump a signal through WTW SOA. Switching points are the points of specific lengths and specific currents at which the power shot down.

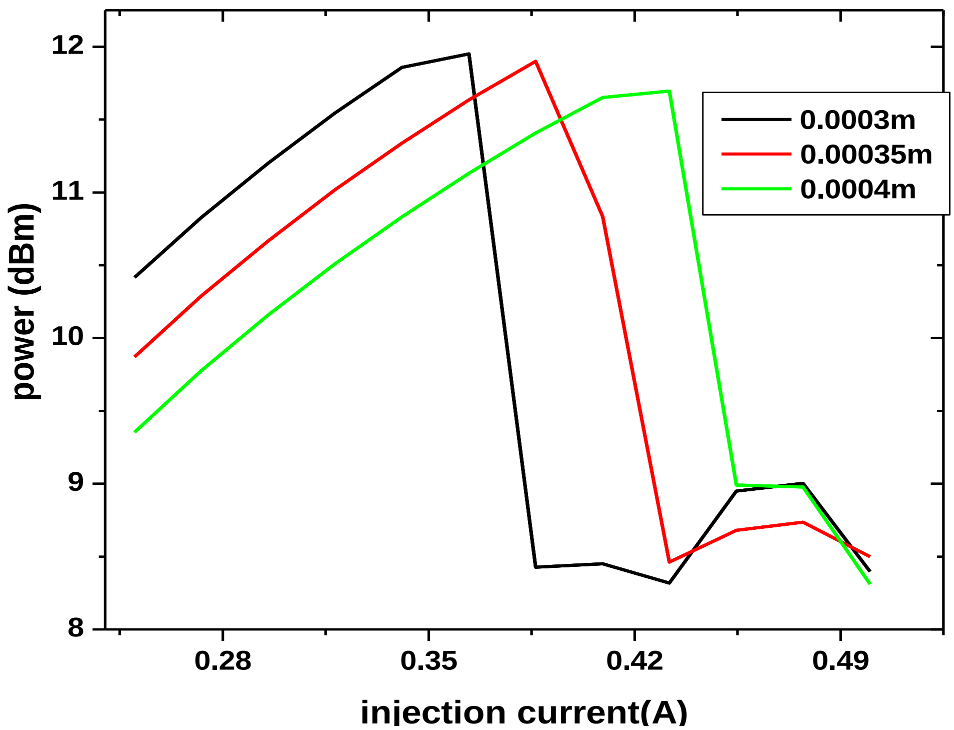

Fig. 4.2: Switching points for the WTW SOA for different lengths

From Fig 4.2, we see that the WTW SOA can make a switch within a range of current 0.35 to 0.45 A for all lengths simulated. The choice for 0.35 - 0.45 A was after simulations for a range for the lowest and highest possible values of currents (0.1- 0.5 A) for WTW SOA for several lengths as shown in Fig B 1 (Appendix B) . For 0.0003 m, there is maximum power output of 11.9817 dBm at injection current I = 0.35636 A. The lengths 0.00035 m and 0.0004 m were noted also to give the best switching points within the shortest time after 0.0003 m. All the lengths simulated as shown in Fig 4.2 showed that power shot down for the range from 0.35 to 0.45 A. Similar switching points were also observed for the lengths; 0.0005 m and 0.0006 m as seen in Fig 4.3. The highest powers of 12.313 dBm and 12.245 dBm were dissipated and was proportional to the input power of -2.8 dBm from the pump CW laser. The lengths were cascaded to assist in obtaining the gates.The switching points shift to higher injection currents when the pupm power was reduced as seen from Fig 4.2 and Fig 4.3.

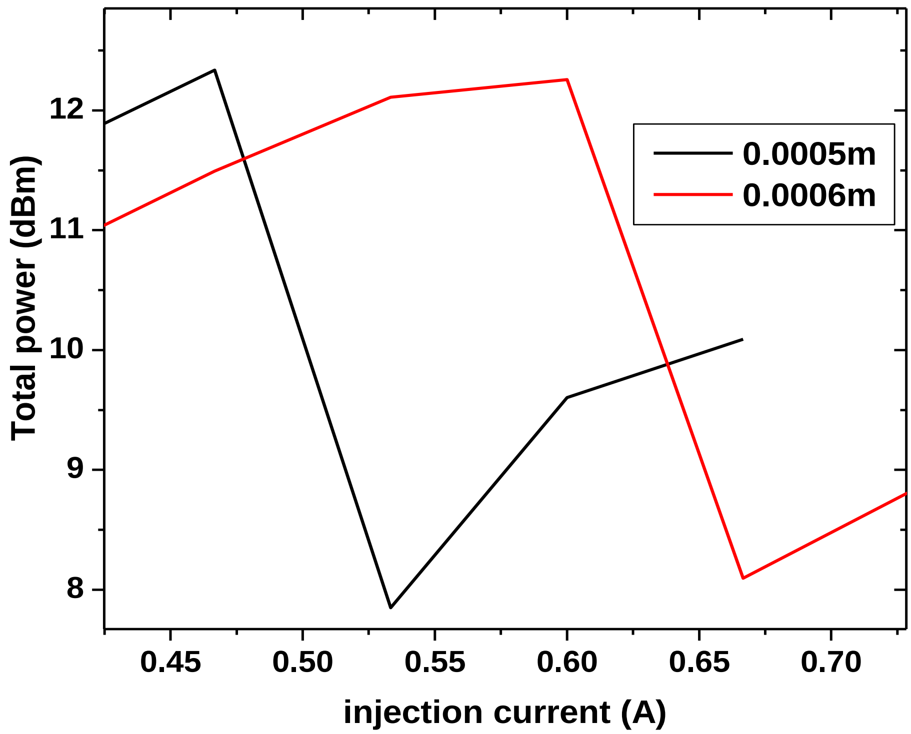

Fig. 4.3: Switching points for selected lengths at -2.8dBm.

4.3 The Inverter (NOT-gate) switch

A modulated signal from transmitter (TX) with 0 dBm light at 1552.524 nm is injected through an optical fibre of length 5 km. The signal was filtered to remove noise before being amplified by EDFA controlled at 10 m as shown in Fig 4.4. The length of the WTW SOA was varied at controlled current of 0.13 A to realize the NOT gate. Light from CW was used to inject the signal and prevent any feedback from the SOA. Both input and output signals were studied using the optical oscilloscope and the results were analyzed using the Origin software and interpreted.

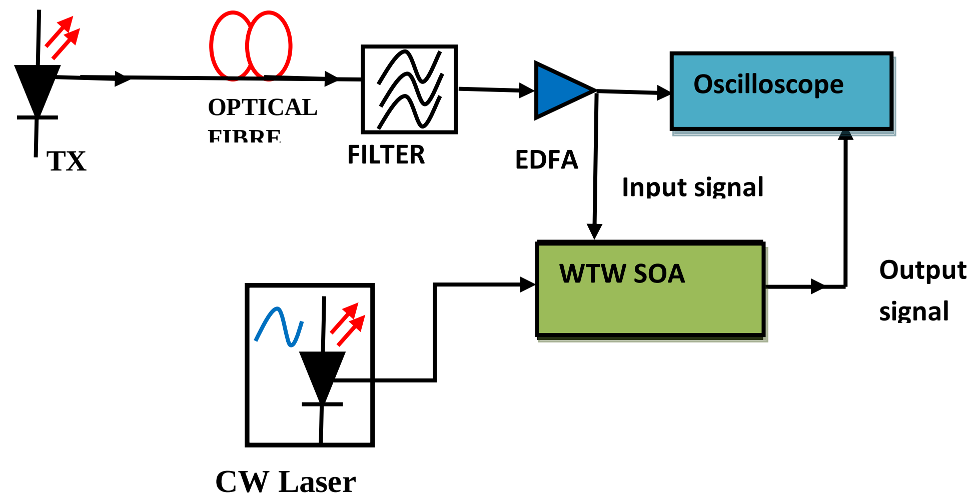

Fig. 4.4: set up for inverter

The results from the simulated inverter in Fig 4.4 are shown in Fig 4.5. It was observed that there was inversion of the input signal in all the lengths.

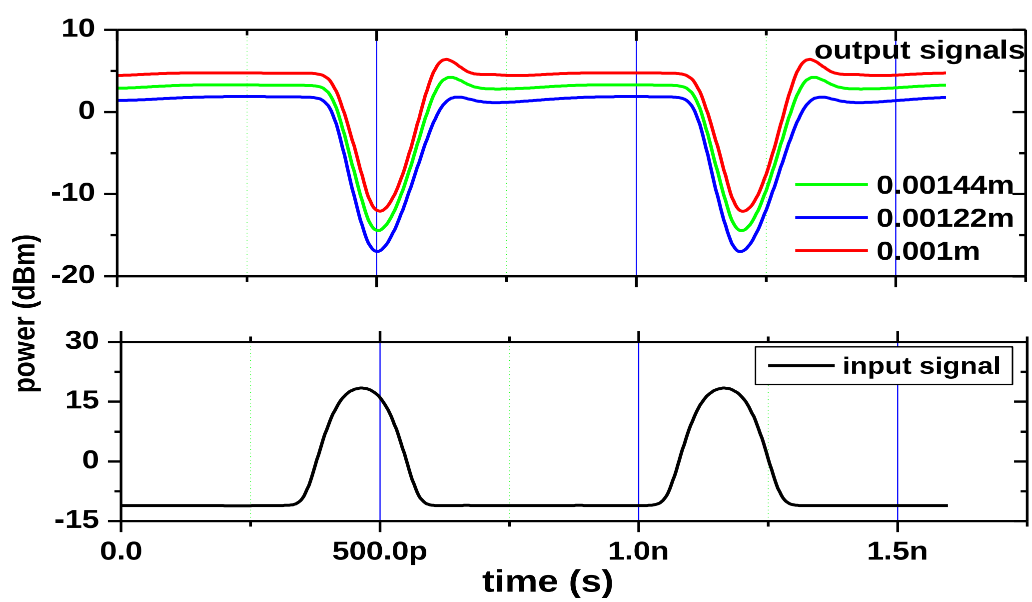

Fig.4.5: Inverter at different lengths for the WTW SOA. It shows variation of power (dBm) against time(s)

The highest power was obtained at 0.001 m as shown in Fig 4.5 while the lowest power was given by 0.00122 m at WTW SOA injection current of 0.13 A. The highest Output signal was distorted as length increased due to the noise that was constantly produced at an average value of -40 dBm. The WTW SOA can then be used to make an inverter. The input signal from the fibre was inverted regardless of length of the SOA.

4.4 The AND-gate switch

The 10 GB/s signal was generated and passed through fibre 1 of length 2 km as shown in Fig 4.6. The signal was split into two channels, where it was optically delayed by optical fibre 2 by varying the length to 2 km before they were coupled at coefficient of 0.5. Attenuator (ATT) and polarization controllers (PC1) and (PC2) were adjusted so that the average powers in input A and input B are equal before the WTW SOA. Synchronized and overlapping signal inputs to WTW SOA were obtained by varying the length of fibre 3.

The length and the currents of WTW SOA were varied, output signals combined and filtered (Gaussian Optical Filter (GOF) was used) at a bandwidth of 3.5 GHz to eliminate noise. The inputs and outputs were visualized using the optical oscilloscope and results analyzed and interpreted.

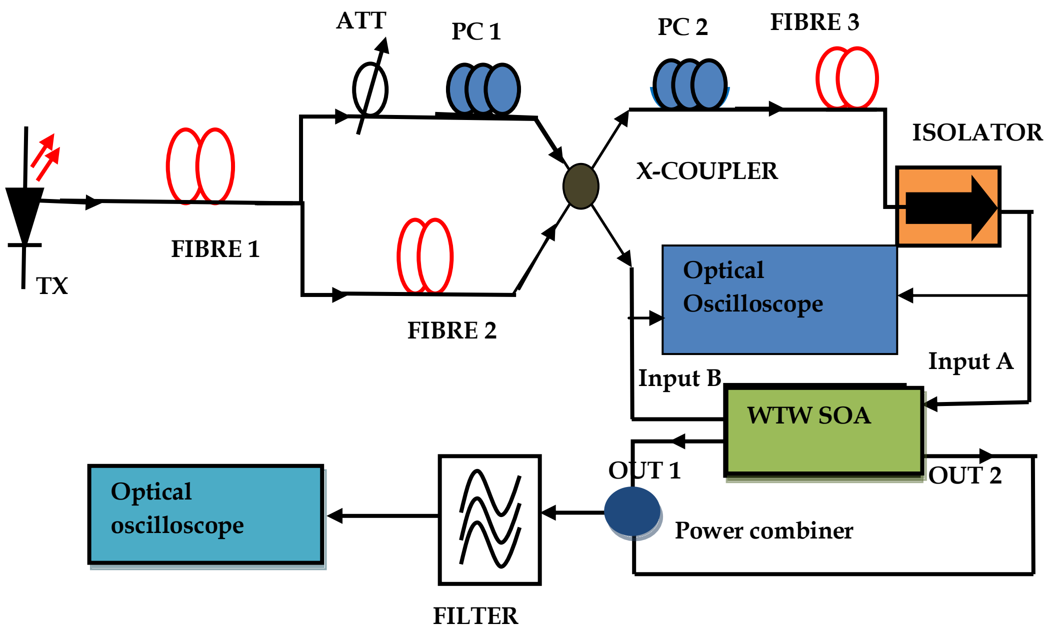

Fig. 4.6: Set up for the AND gate

The simulated results for the AND gate in Fig 4.6 are shown in Fig 4.7 for different lengths for pump power of 0 dBm from CW laser.

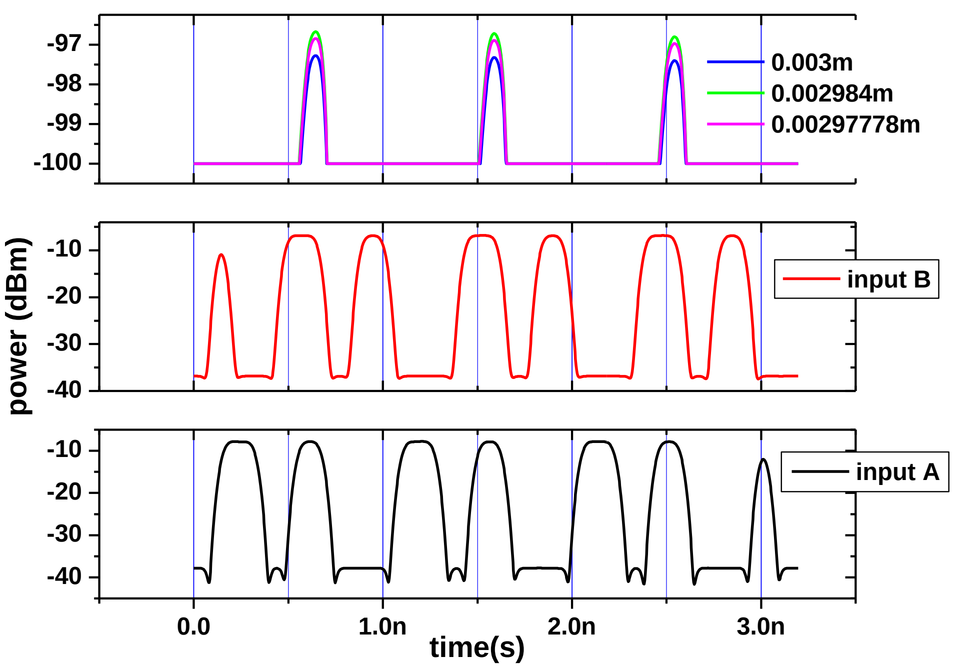

Fig. 4.7: AND gate at different lengths.

It was observed that, as the length of the SOA increased the AND gate is build i.e. from lengths 0.00297778 m to nearly 0.004 m. The power dissipated decreases significantly before the signal 'died off' at -100 dBm. When the input length at one channel was 1 km (low) and 2 km (high) on the other channel, the AND gate was realized at length of 0.003 m in SOA as shown in Fig 4.7. This ment that for the logic inputs where at one channel, the signal was HIGH and LOW on the other channel, the output was LOW. If on both channels its HIGH the output was HIGH. If it was LOW on both channels, the output will be LOW. This relationship of AND gate corresponds well to the theory. In summary, WTW SOA worked well at length of 0.003 m for injection current of 0.0003 A as AND gate. Further research for the combination of AND gate and the inverter can be undertaken in future to realize the NAND gate.

4.5 The OR gate switch

A signal pattern was generated and injected through optical fibre1 of 1 km as shown Fig 4:8. The signal was split into two; one signal through the Attenuator (ATT1), Polarization Combiner (PC1) and the other signal through an Optical fibre2 at length of 2 km and PC2. The ATT and PC were adjusted to obtain the average power. Coupling of the signals were done at coefficient of 0.5. This was to attain signals of similar characteristics being propagated in both channels. The signal was amplified using EDFA1 of length 15 m as input B and also passed through PC and Optical fibre 3 of length 4.5 km and EDFA2 of length 15 m as input A. The injection current in the WTW SOA was 3.1 mA and the length was varied to obtain the power combined outputs which were amplified using the Optical amplifier (AMP) at gain factor of 50 dBm and Noise factor of 1 for clarity and filtered at bandwidth of 50 GHz to eliminate noise. The resultant output signal was visualized using the Oscilloscope and results were interpreted.

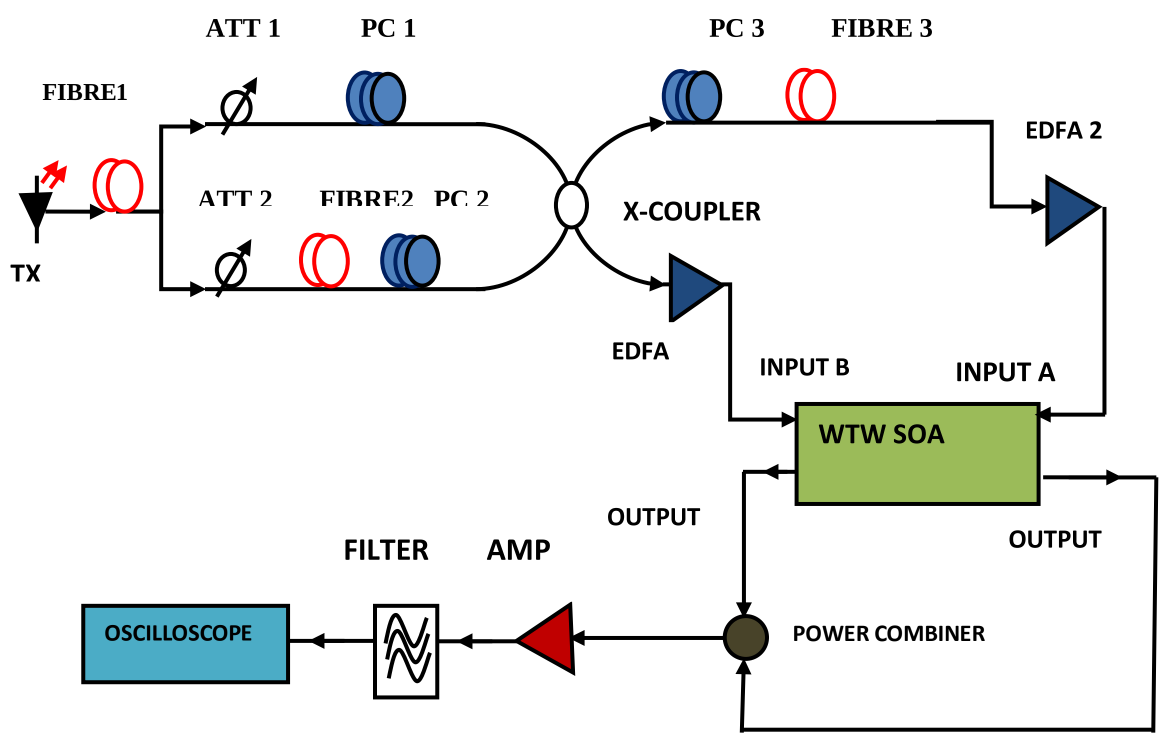

Fig. 4.8: The set-up for the OR gate

After the simulation it was observed that OR gate builds at different lengths as shown in Fig 4.9.

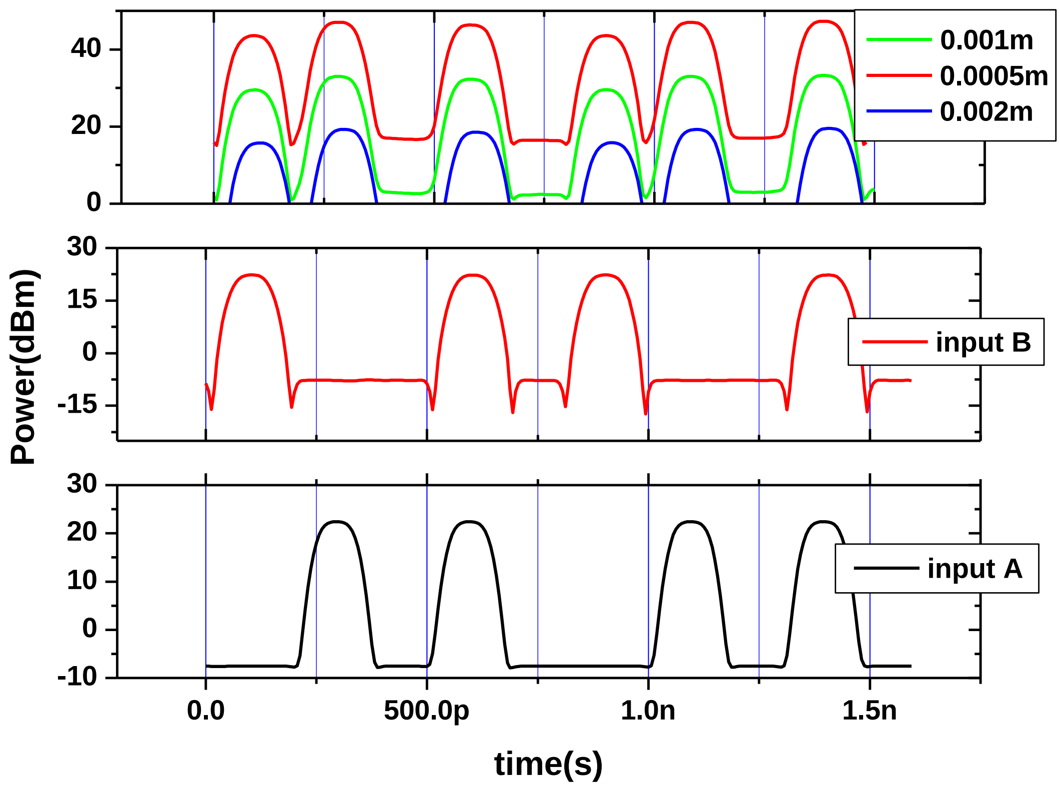

Fig. 4.9: OR gate at various lengths showing amount of power dissipated

The values for the various lengths clearly showed that, inputs fed to the SOA results to OR gate. The highest power was dispelled at lowest value length of 0.0005 m while 0.002 m had a small power output. This showed that, the OR gate was realized with decrease in length with power in WTW SOA at controlled injection current of 0.0031 A. Phase shift was witnessed when the signal passed through the components of the connected inverter i.e on exiting the fibre. This clearly showed that, from the inputs where there was HIGH signal on one arm or LOW signal on the other arm of the input, the results was HIGH. If both are LOW, it was seen to give LOW, if both are HIGH, the result was HIGH. The amount of power dissipated was noted to reduce as the length of the WTW SOA OR gate reduced. This was due to the noise from the components resulting to the signal distortion beyond -100 dBm. This was a feature which was also noted in the AND gate.

CHAPTER FIVE

CONCLUSIONS AND RECOMMENDATIONS

5.1 Conclusions

Optical gates NOT, AND and OR have been successfully modeled and demonstrated using WTW SOA. WTW SOA has been successfully used by simulation to create different switching points at different lengths and different injection currents. The measuring of the output power against different injection currents at different lengths resulted to the optical gates. The NOT gate, signal inversion was obtained at 0.001m and current of 0.13 A. The input signal inversion occurred at any length of the WTW SOA. The AND gate was build specifically at length of 0.003 m. The current of the WTW SOA then was 0.0003 A. The OR gate was obtained from the WTW SOA current 0.0031A at small value length of 0.0000001 m , 0.0005 m, 0.001 m and 0.002 m.

5.2 Recommendations

The setups used for the obtained optical gates are easy to implement and therefore challenges encountered in optical communication and computing networks can be addressed. The obtained results need experimental validation since they were not at the end of this research. Further research needs to be done to obtain NOR, NAND, EXNOR and EXOR gates. All the obtained gates are important in optical signal processing, computer and communication networks since it performs the logic functions such as: signal integration, time reversals, differentiation and multiplexing. Others are automatic switching for routing, wavelength conversion, data generation and regeneration. The optical gates functions can eliminate data delay and traffic along the communication network.

REFERENCES

Acosta, M. C., Maldonado, R., & Soto, H. (2008, November). Degradation by the cross-polarization modulation of the conversion efficiency of a wavelength converter based on FWM in a SOA. In *Asia Pacific Optical Communications* (pp. 713526-713526). International Society for Optics and Photonics.

Agrawal, G. P. *Nonlinear Fibre Optics*, Academic Press, San Diego, Third Edition, 2001, Chap.2

Agrawal, G. P. (2012). *Fibre-optic communication systems* (Vol. 222). New York, John Wiley & Sons.

Barnoski, M. (Ed.). (2012). *Fundamentals of optical fibre communications*. Elsevier.

Baveja, P. P., Maywar, D. N., & Agrawal, G. P. (2012). Interband four-wave mixing in semiconductor optical amplifiers with ASE-enhanced gain recovery. *Selected Topics in Quantum Electronics, IEEE Journal of*, *18*(2), 899-908.

Baveja, P. P., Maywar, D. N., Kaplan, A. M., & Agrawal, G. P. (2010). Self-phase modulation in semiconductor optical amplifiers: impact of amplified spontaneous emission. *Quantum Electronics, IEEE Journal of*, *46*(Jarvinen *et al.*), 1396-1403.

Berrettini, G., Simi, A., Malacarne, A., Bogoni, A., & Poti, L. (2006). Ultrafast integrable and reconfigurable XNOR, AND, NOR, and NOT photonic logic gate. *Photonics Technology Letters, IEEE*, *18*(8), 917-919.

Buck, J. A. (2004). *Fundamentals of optical fibres*. John Wiley & Sons.

Choi, K. S., Byun, Y. T., Lee, S., & Jhon, Y. M. (2010). All-optical OR/NOR bi-functional logic gate by using cross-gain modulation in semiconductor optical amplifiers. *Journal of the Korean Physical Society*, *56*(4), 1093-1096.

Connelly, M. J. (2001). Wideband semiconductor optical amplifier steady-state numerical model.

Gates, A. O. (2012). Semiconductor Optical Amplifiers (SOA) Performance Optimization in Optical Communication System. *3* (9), 2229-3345.

Guan, Y., Wang, R., Chen, X., Zhang, Z., Duan, Z., & Chen, C. (2013). A Method to Implement Data Extraction Using and Optical Gate Based on SOR-NOLM.

Guo, L. Q., & Connelly, M. J. (2005, August). All-optical AND gate using nonlinear polarization rotation in a bulk semiconductor optical amplifier. In *Optical Amplifiers and Their Applications* (p. SuB9). Optical Society of America.

Hedekvist, P. O., Bhardwaj, A., Vahala, K., & Andersson, H. (2001). Advanced all-optical logic gates on a spectral bus. *Applied optics*, *40*(11), 1761-1766.

Hong, Y., Spencer, P. S., & Shore, K. A. (2004). Wide-band polarization-free wavelength conversion based on four-wave-mixing in semiconductor optical amplifiers. *Quantum Electronics, IEEE Journal of*, *40*(2), 152-156.

Houbavlis, T., Zoiros, K., Vlachos, K., Papakyriakopoulos, T., Avramopoulos, H., Girardin, F., & Burkhard, H. (1999). All-optical XOR in a semiconductor optical amplifier-assisted fibre Sagnac gate. *IEEE Photonics Technology Letters*, *11*(3), 334-336.

Ientilucci, E. (1993). Fundamentals of Fibre Optics.

Kadam, B., & Gupta, N. (2012). All optical xor gate using single soa at 100 GB/s. *International Journal of Computational Intelligence Techniques*, *3*(2), 86-89.

Kang, B. K., Kim, J. H., Byun, Y. T., Lee, S., Jhon, Y. M., Woo, D. H., & Yu, B. G. (2002). All-optical AND gate using probe and pump signals as the multiple binary points in cross phase modulation. *Japanese journal of applied physics*, *41*(5B), L568.

Kaur, S., & Kaler, R. S. (2014). 5 GHz all-optical binary counter employing SOA-MZIs and an optical NOT gate. *Journal of Optics*, *16*(3), 035201.

Kim, J. H., Kim, Y., Byun, Y. T., Jhon, Y. M., Lee, S., Kim, S. H., & Woo, D. H. (2004). All-optical logic gates using semiconductor optical-amplifier-based devices and their applications. *J. Korean Phys. Soc*, *45*(7), 1158-1161.

Kleinberg, J., & Kumar, A. (2001). Wavelength conversion in optical networks. *Journal of algorithms*, *38*(Jarvinen *et al.*), 25-50.

Li, Z., Liu, Y., Zhang, S., Ju, H., De Waardt, H., Khoe, G. D., & Lenstra, D. (2005, September). All-optical logic gates based on an SOA and an optical filter. In *31st European Conference on Optical Communication* (Vol. 2, pp. 229-230).

Li, Z., Liu, Y., Zhang, S., Ju, H., De Waardt, H., Khoe, G. D., & Lenstra, D. (2005). All-optical logic gates using semiconductor optical amplifier assisted by optical filter. *Electronics Letters*, *41*(25), 1397-1399.

Liu, Y., Tangdiongga, E., Li, Z., De Waardt, H., Koonen, A. M. J., Khoe, G. D., ... & Dorren, H. J. S. (2007). Error-free 320-GB/s all-optical wavelength conversion using a single semiconductor optical amplifier. *Journal of Lightwave Technology*, *25*(Jarvinen *et al.*), 103-108.

Manning, R. J., Giller, R., Yang, X., Webb, R. P., & Cotter, D. (2007, July). SOAs for all-optical switching-techniques for increasing the speed. In *9th International Conference on Transparent Optical Network (ICTON), Rome, Italy* (pp. 1-5).

Massaro, A. (2012). Photonic Crystals: Introduction, Applications and Theory. *InTech, Croatia*.

Patil, C. V., Singh, D., & Singh, B. (2014). Analysis of Optical Logic Gates Based on SOA. *International Journal of Electrical, Electronics and Computer Engineering*, *3*(2), 30.

Qiu, J., Sun, K., Rochette, M., & Chen, L. R. (2010). Reconfigurable all-optical multilogic gate (XOR, AND, and OR) based on cross-phase modulation in a highly nonlinear fibre. *Photonics Technology Letters, IEEE*, *22*(16), 1199-1201.

Said, Y., & Rezig, H. (2011). SOAs Nonlinearities and Their Applications for Next Generation of Optical Networks. *Sys' Com Laboratory, National Engineering School of Tunis (ENIT) Tunisia*.

Sahafi, M., Rostami, A., & Sahafi, A. (2012). All-optical high speed logic gates using SOA. *Optics Communications*, *285*(Jarvinen *et al.*), 2289-2292.

Said, Y., Rezig, H., & Bouallegue, A. (2010). Performance Evaluation of Wavelength Conversion Using a Wideband Semiconductor Optical Amplifier at 40 Gbit/s. *Open Optics Journal*, *4*, 21-28.

Saleh, B. E., Teich, M. C., & Saleh, B. E. (1991). *Fundamentals of photonics* (Vol. 22). New York: Wiley.

Sarkar, P. P., & Mukhopadhyay, S. (2014). All optical frequency encoded NAND logic operation along with the simulated result. *Journal of Optics*, *43*(3), 177-182.

Saxena, S. S. (2015). Realization of all-optical NOR gate based on four wave mixing, non-linear effect in SOA. *International Journal of Latest Trends in Engineering and Technology (IJLTET) , 5* (1), 138-144.

Singh, P., Tripathi, D. K., Jaiswal, S., & Dixit, H. K. (2014). All-Optical Logic Gates: Designs, Classification, and Comparison. *Advances in Optical Technologies*, *2014*.

Son, C. W., Kim, S. H., Jhon, Y. M., Byun, Y. T., Lee, S., Woo, D. H., ... & Yoon, T. H. (2007). Realization of all-optical XOR, NOR, and NAND gates in single format by using semiconductor optical amplifiers. *Japanese journal of applied physics*, *46*(1R), 232.

Stevan Jr, S., & Teixeira, A. (2014). Experimental Analysis of an All Optical NOT Gate and Latch based on an Externaly Clamped Semiconductor Optical Amplifier. *Journal of Communication and Information Systems*, *29*(Jarvinen *et al.*).

Teich, M. C., & Saleh, B. E. A. (1991). Fundamentals of photonics. *Canada, Wiley Interscience*, 3.

Teimoori, H., Apostolopoulos, D., Vlachos, K. G., Ware, C., Petrantonakis, D., Stampoulidis, L., & Erasme, D. (2008). Optical-logic-gate aided packet-switching in transparent optical networks. *Journal of Lightwave Technology*, *26*(16), 2848-2856.

Wang, Y., Wu, C., Shi, X., Yang, S., & Wang, Y. (2009). An all optical xor logic gate for nrz based on TOAD. In *Progress In Electromagnetics Research Symposium], PIERS Proceedings* (pp. 1286-1290).

Wu, J. W., & Sarma, A. K. (2010). Ultrafast all-optical XOR logic gate based on a symmetrical Mach-Zehnder interferometer employing SOI waveguides. *Optics Communications*, *283*(14), 2914-2917.

Yi, L., Hu, W., & He, H. (2010). Reconfigurable multi-logic gates based on SOA nonlinear polarization rotation effect. In *OECC 2010 Technical Digest* (pp. 194-195).

Zhang, M., Zhao, Y., Wang, L., Wang, J., & Ye, P. (2003). Design and analysis of all-optical XOR gate using SOA-based Mach–Zehnder interferometer. *Optics Communications*, *223*(4), 301-308.

Zhang, X., Wang, Y., Sun, J., Liu, D., & Huang, D (2004). Novel all-optical AND gate based on cascaded single-port-coupled SOAs.

Zheng, Q. (2012). On the SOA-based MZI all-optical logic gates for all-optical networks. *arXiv preprint arXiv:1205.0268*.

APPENDIX A

Journal and Conference Publications

1. **Ngetich Wesley**, Waswa David and Matere Isaac, *"Simulation of NOT, AND, OR and NOR Optical Gates Using Wideband Travelling Wave Semiconductor Optical Amplifier (WTW SOA)", vol 5, issue 9,* ISSN 2250-2459,Pg 20-24, September 2015
2. I.M. Matere**, W. Ngetich** and D. W. Waswa, *" Modeling of Ring Resonators for Optical Filters Applications using MEEP" vol 5, issue 9,* ISSN 2250-2459,Pg 14-19, September 2015
3. D. M. Osiemo, D. W. Waswa, K. M. Muguro and **Ngetich Wesley**, *"Stimulated Brillouin Scattering Characterization and Slow Light Generation Technique in Modern Optical Fibres" , vol 5, issue 9,* ISSN 2250-2459,Pg 39-43, September 2015
4. **Ngetich Wesley**, Waswa David and Matere Isaac,*"Simulation of NOT, AND, OR and NOR optical gates using Wideband Travelling Wave Semiconductor Optical Amplifier (WTW SOA)",* University Of Eldoret 1st interdisciplinary Conference*18th – 19th June* 2015

APPENDIX B

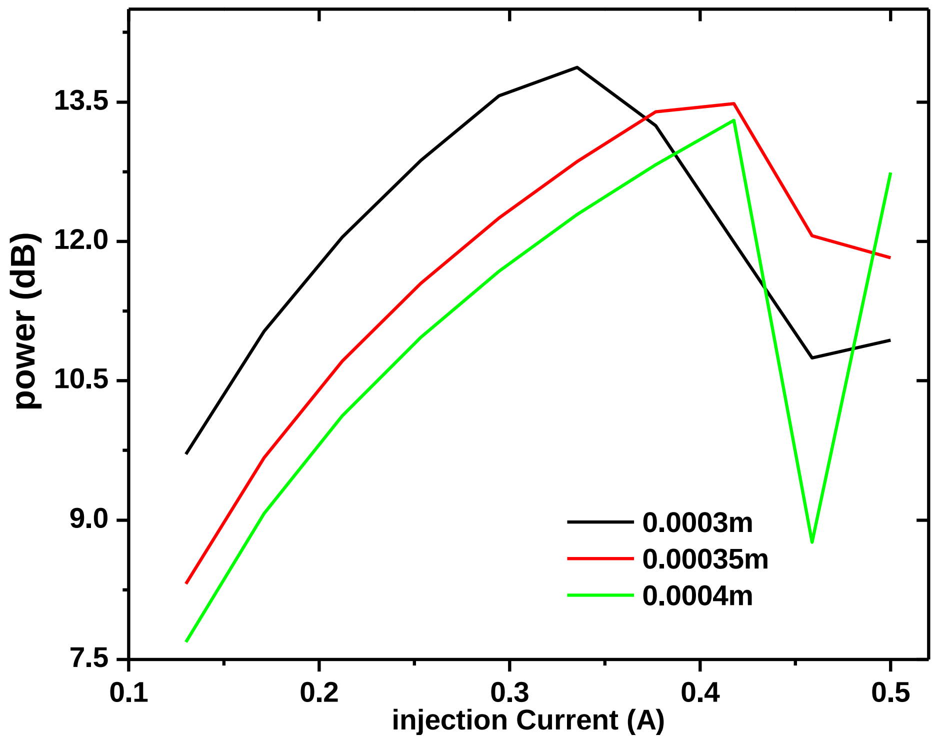

Fig B 1: Switching points for WTW SOA for several lengths for range of current 0.1- 0.5 A